



Antibodies from Rabbits Immunized with HIV-1 Clade B SOSIP Trimers Can Neutralize Multiple Clade B Viruses by Destabilizing the Envelope Glycoprotein

M. M. van Haaren,^a L. E. McCoy,^{b,c} J. L. Torres,^d W. Lee,^d C. A. Cottrell,^d J. L. Copps,^d P. van der Woude,^a A. Yasmeeen,^e S. W. de Taeye,^a A. Torrents de la Peña,^a J. P. Moore,^e D. R. Burton,^{b,f,g} P. J. Klasse,^e A. B. Ward,^{d,f,g} R. W. Sanders,^{a,e} M. J. van Gils^a

^aDepartment of Medical Microbiology, Amsterdam Infection & Immunity Institute, Amsterdam UMC, location AMC, University of Amsterdam, Amsterdam, The Netherlands

^bDepartment of Immunology and Microbiology, The Scripps Research Institute, La Jolla, California, USA

^cDivision of Infection and Immunity, University College London, London, United Kingdom

^dDepartment of Integrative Structural and Computational Biology, The Scripps Research Institute, La Jolla, California, USA

^eDepartment of Microbiology and Immunology, Weill Medical College of Cornell University, New York, New York, USA

^fInternational AIDS Vaccine Initiative–Neutralizing Antibody Center (IAVI-NAC), The Scripps Research Institute, La Jolla, California, USA

^gCenter for HIV/AIDS Vaccine Development (CHAVD), The Scripps Research Institute, La Jolla, California, USA

ABSTRACT The high viral diversity of HIV-1 is a formidable hurdle for the development of an HIV-1 vaccine. Elicitation of broadly neutralizing antibodies (bNAbs) would offer a solution, but so far immunization strategies have failed to efficiently elicit bNAbs. To overcome these obstacles, it is important to understand the immune responses elicited by current HIV-1 envelope glycoprotein (Env) immunogens. To gain more insight, we characterized monoclonal antibodies (MAbs) isolated from rabbits immunized with Env SOSIP trimers based on the clade B isolate AMC008. Four rabbits that were immunized three times with AMC008 trimer developed robust autologous and sporadic low-titer heterologous neutralizing responses. Seventeen AMC008 trimer-reactive MAbs were isolated using antigen-specific single B-cell sorting. Four of these MAbs neutralized the autologous AMC008 virus and several other clade B viruses. When visualized by electron microscopy, the complex of the neutralizing MAbs with the AMC008 trimer showed binding to the gp41 subunit with unusual approach angles, and we observed that their neutralization ability depended on their capacity to induce Env trimer dissociation. Thus, AMC008 SOSIP trimer immunization induced clade B-neutralizing MAbs with unusual approach angles with neutralizing effects that involve trimer destabilization. Optimizing these responses might provide an avenue to the induction of trimer-dissociating bNAbs.

IMPORTANCE Roughly 32 million people have died as a consequence of HIV-1 infection since the start of the epidemic, and 1.7 million people still get infected with HIV-1 annually. Therefore, a vaccine to prevent HIV-1 infection is urgently needed. Current HIV-1 immunogens are not able to elicit the broad immune responses needed to provide protection against the large variation of HIV-1 strains circulating globally. A better understanding of the humoral immune responses elicited by immunization with state-of-the-art HIV-1 immunogens should facilitate the design of improved HIV-1 vaccine candidates. We identified antibodies with the ability to neutralize multiple HIV-1 viruses by destabilization of the envelope glycoprotein. Their weak but consistent cross-neutralization ability indicates the potential of this epitope to elicit broad responses. The trimer-destabilizing effect of the neutralizing MAbs, combined with detailed characterization of the neutralization epitope, can be used to shape the next generation of HIV-1 immunogens to elicit improved humoral responses after vaccination.

KEYWORDS HIV-1, vaccine, monoclonal antibodies, AMC008 SOSIP, trimer destabilization, approach angle, human immunodeficiency virus

Citation van Haaren MM, McCoy LE, Torres JL, Lee W, Cottrell CA, Copps JL, van der Woude P, Yasmeeen A, de Taeye SW, Torrents de la Peña A, Moore JP, Burton DR, Klasse PJ, Ward AB, Sanders RW, van Gils MJ. 2021. Antibodies from rabbits immunized with HIV-1 clade B SOSIP trimers can neutralize multiple clade B viruses by destabilizing the envelope glycoprotein. *J Virol* 95:e00094-21. <https://doi.org/10.1128/JVI.00094-21>.

Editor Guido Silvestri, Emory University

Copyright © 2021 van Haaren et al. This is an open-access article distributed under the terms of the [Creative Commons Attribution 4.0 International license](https://creativecommons.org/licenses/by/4.0/).

Address correspondence to R. W. Sanders, R.W.Sanders@amsterdamumc.nl, or M. J. van Gils, M.J.vangils@amsterdamumc.nl.

Received 17 February 2021

Accepted 19 May 2021

Accepted manuscript posted online 2 June 2021

Published 10 August 2021

The ongoing HIV-1 epidemic, in spite of effective HIV-1 medication, highlights the need for an HIV-1 vaccine. To achieve this goal, knowledge of the immune responses elicited by state-of-the-art HIV-1 immunogens is important. Such knowledge will allow the further optimization and development of these immunogens. Many immunogens that are being explored as subunit vaccines are based on the HIV-1 envelope glycoprotein (Env) trimer (1–6). The Env trimer is the only viral protein expressed on the outside of the HIV-1 particle and therefore the only target for neutralizing antibodies (NAbs). Because circulating HIV-1 viruses have extremely diverse Env sequences, in order to provide protection, an HIV-1 vaccine needs to induce broadly neutralizing antibodies (bNAbs), i.e., NAbs that can cope with Env diversity (7). Extensive research has provided the field with soluble, stable, and native-like versions of Env, including SOSIP trimers (8). So far, SOSIP trimers have generally elicited strong autologous NAb responses, but only sporadic, inconsistent, and weak cross-NAb responses (9–12). It is imperative to study these antibody (Ab) responses to understand precisely which improvements are needed to consistently broaden the response. Iterative vaccine design based on monoclonal Abs (MAbs) isolated from vaccinated animals is a valuable way to overcome the limitations of the current HIV-1 immunogens (13, 14).

Previous studies characterizing MAbs and bulk serum of SOSIP Env trimer-immunized rabbits and macaques showed that the Ab responses frequently target strain-specific glycan holes (15–17). Indeed, the immunodominance of glycan holes was confirmed by redirection of vaccine-induced Ab responses toward *de novo* glycan holes when the original strain-specific glycan hole was filled (18). Env trimers from different virus isolates probably have their own specific immunodominant glycan holes, which would explain why Env trimer-immunized animals develop very limited neutralization breadth. Another immunodominant region after immunization is the unprotected base of the soluble Env trimer (17, 19, 20). This region of the Env trimer is, in its natural display, concealed by the viral membrane and in no need of heavy glycosylation to evade the immune system. However, on soluble Env trimers, the base forms a large glycan hole that is easily accessed by the immune system, and induces Abs that cannot recognize the full-length Env trimer, i.e., that are non-NAbs.

Many vaccine-induced NAbs target epitopes that overlap those of non-NAbs (11, 15, 16). Yet, it is unclear what exactly determines whether an Ab will have neutralizing ability. For some Ab families, binding kinetics might influence neutralization ability (21, 22). Indeed, it has been shown that some Ab families elicited during natural infection have kinetics of Ab binding that correlate with their neutralization ability. In particular, a high off-rate constant was associated with absent or less effective neutralization. The on-rate constant and overall affinity appeared to be of less influence on the ability to neutralize (21, 22).

SOSIP-induced NAbs have been discovered that target the same epitope as well-known bNAbs elicited after natural HIV-1 infection, but without displaying the same potency or breadth (17, 19, 23–25). Some studies have shown that the approach angle is relevant in this respect. For instance, for CD4-binding site (CD4bs)-directed Abs, the correct approach angle is essential for their ability to neutralize. The right approach angle allows bNAbs to reach the CD4bs while circumventing the dense Env glycan shield (23).

Several vaccines involving state-of-the-art Env trimer immunogens (1, 10) or specific Env epitope scaffolds (26, 27) have induced sporadic NAb responses against heterologous viruses in addition to autologous NAbs. Although such heterologous neutralization can be broad, spanning many clades, it is usually not very potent. Interestingly, two bNAbs have been isolated from a rabbit immunized with Env trimers on liposomes (1). This rabbit serum exhibited broad neutralization, and the isolated bNAbs recapitulated that activity. The development of breadth in this one rabbit was exceptional, as none of the other rabbits receiving the same immunogens developed this remarkable neutralization breadth, but the detailed characterization of such immune responses through the isolation of MAbs helps to understand why the development of neutralization breadth is rare and how it can be improved.

In this study, we isolated MAbs from four rabbits immunized with the clade B Env trimer immunogen AMC008 SOSIP. We identified an immunodominant area on the gp41 subunit of the AMC008 SOSIP trimer. Interestingly, these NAbs could cross-neutralize other clade B viruses. Negative-stain electron microscopy (NS-EM) revealed that these NAbs bound with an unusual approach angle that would be expected to be incompatible with binding to virus-associated Env trimers because of a clash with the viral membrane. Contrary to expectations and despite the unusual angle of approach, these MAbs were able to bind and neutralize, demonstrating remarkable flexibility of virus-associated Env trimers in their interaction with Abs (28). We further showed that the neutralization capacity of these NAbs depended on their ability to dissociate the Env trimer, similarly to what has been described previously for bNAbs isolated from both humans and rabbits (1, 29). The information gathered from this study helps to elucidate mechanistic aspects of virus neutralization and may help to tailor immunogens to elicit trimer-dissociating NAbs.

RESULTS

AMC008 SOSIP immunization induces NAbs and non-NAbs. In a previous study by our group, 15 rabbits (animal identifiers 1594 to 1608) were immunized with the clade B Env trimer AMC008 SOSIP (10). This immunogen was based on the viral sequence from an individual enrolled in the Amsterdam Cohort Studies (ACS) that showed broad serum neutralization (10). All AMC008 SOSIP trimer-immunized rabbits showed consistent autologous neutralization, as well as low cross-neutralization of the clade B viruses BaL, REJO, WITO, and SHIV162p3 (10). We further investigated serum neutralization of animals 1605 to 1608 and observed cross-neutralization at low titers by two and four rabbits, respectively, of the clade B viruses AMC009 and AMC018, isolated from different HIV-infected individuals (Fig. 1A). To better understand the cross-neutralization in these animals and its limitations, MAbs were isolated from these four AMC008 SOSIP trimer-immunized rabbits. Peripheral blood mononuclear cells (PBMCs) were obtained from these animals at week 21, 1 week after the third immunization (Fig. 1A). Single B cells expressing IgG, and with the ability to bind two distinctly labeled fluorescent AMC008 SOSIP trimers, were selected by fluorescence-activated cell sorting (FACS). On average, 5% of total live B cells were AMC008 SOSIP trimer reactive. B-cell receptor (BCR) sequences were subsequently amplified and cloned into expression vectors to generate MAbs that were tested for binding to autologous AMC008 SOSIP trimers by enzyme-limited immunosorbent assay (ELISA). A total of 17 MAbs bound the AMC008 SOSIP trimer. Rabbits 1605 and 1607 yielded 7 and 8 MAbs, respectively, while from the other two rabbits (1606 and 1608), only one MAb each was generated (Fig. 1B).

Sequence analysis of the heavy chain variable region showed the expected polyclonal immune response within each rabbit (Fig. 1C). From these sequences, we determined the length of the complementary determining region 3 of the heavy and the light chains (CDRH3 and CDRL3, respectively). The CDRH3 is important, as it interacts directly with the immunogen and is often elongated in human bNAbs to cope with the extensive glycan shield surrounding the Env trimer (30, 31). We also analyzed the CDRL3 because rabbit Abs, in contrast to human Abs, usually interact with the immunogen predominantly through the CDRs of their light chain (32). The average length of the CDRH3 of all AMC008 SOSIP trimer-reactive MAbs was 15 amino acids, which agrees with previous studies on CDRH3 lengths of BCR sequences in naive rabbits (32, 33) (Fig. 1D). However, the individual CDRH3 length varied greatly, ranging from 10 to 22 amino acids. The average CDRL3 length was increased with 2-amino-acid residues to an average of 14 residues in AMC008 SOSIP trimer-reactive MAbs from 12 residues in BCR sequences from naive rabbits (32, 33). The distribution of the individual CDRL3 lengths in the rabbits was more limited than that of the CDRH3 region, ranging from 11 to 16 amino acids (Fig. 1D).

We then tested the isolated MAbs for their ability to neutralize the autologous AMC008 virus (Fig. 1E). Four of the 17 MAbs were able to neutralize the AMC008 virus, although with relatively low potency (50% inhibitory concentration [IC_{50}] values ranging

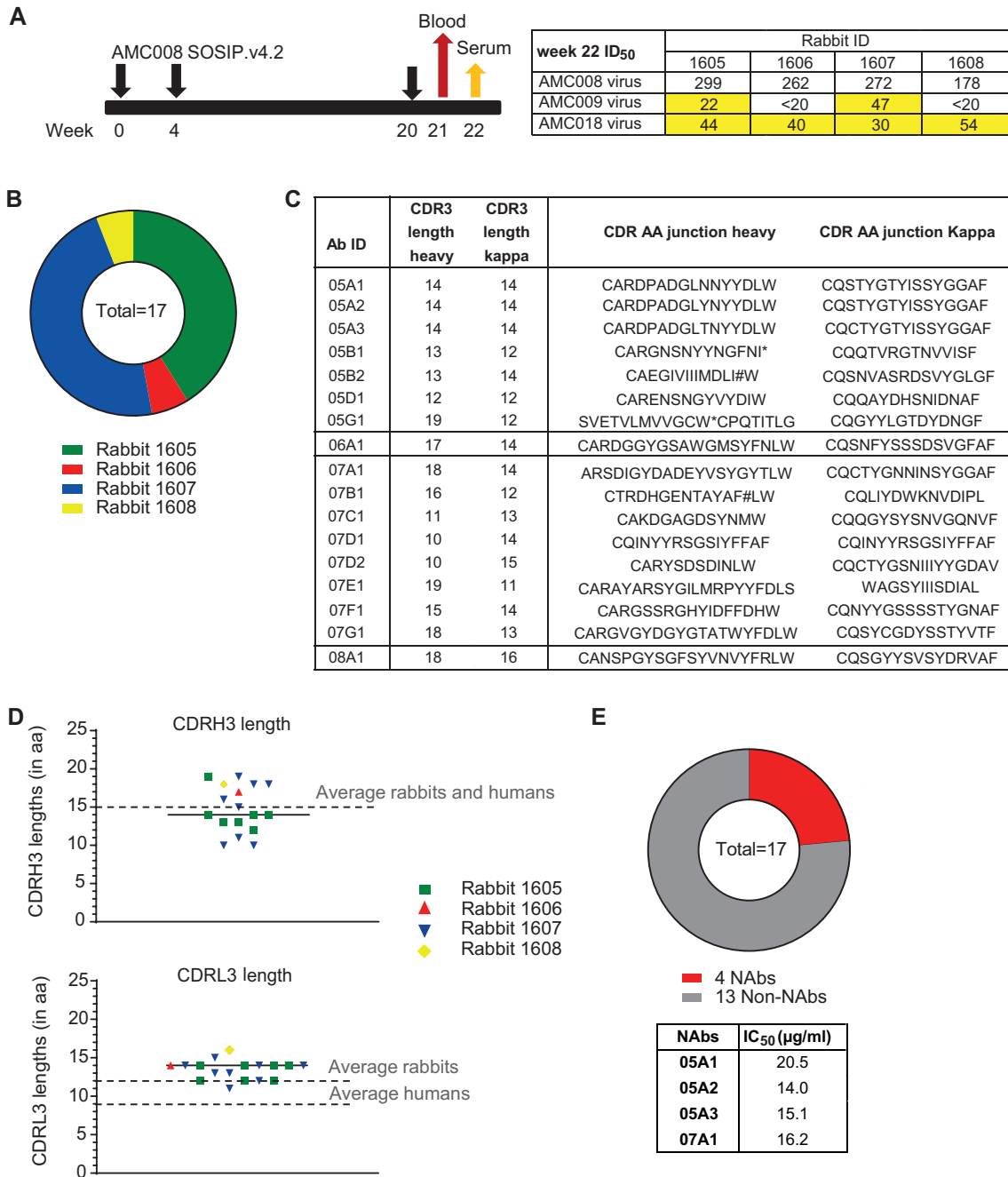


FIG 1 Characteristics of monoclonal antibodies (MAbs) isolated from AMC008 SOSIP trimer-immunized rabbits. (A) Immunization and sample collection scheme (left) and autologous and heterologous serum neutralization titers at week 22 (right) for four AMC008 SOSIP trimer-immunized rabbits. Serum neutralization 50% infective dose (ID₅₀) is shown for each animal. (B) Absolute number of MAbs isolated per animal. (C) Individual CDR3 lengths and CDR amino acid junction sequence of heavy and light chains of all isolated MAbs. (D) Individual CDR3 amino acid lengths of the isolated MAbs. (E) Autologous neutralization ability of the isolated MAbs. Neutralization 50% inhibitory concentration (IC₅₀) values are shown for each of the four neutralizing antibodies (NABs) in the accompanying table.

from 16 to 19 µg/ml). Three of the identified four NABs were isolated from rabbit 1605 and belonged to the same clonal family; these were designated 05A1, 05A2, and 05A3. The fourth NAB was isolated from rabbit 1607 and named 07A1. Alignment of heavy and light chain variable regions revealed 93% sequence similarity between the CDRL3 sequences of the 05A family (Fig. 1C). In addition, we found no evidence of gene conversion, a common feature for rabbit Abs, within this family of 3 MAbs. Interestingly, NAb

TABLE 1 Heterologous binding ability of the isolated NABs^a

	Antibody ID	Clade	Tier	05A1	05A2	05A3	07A1
Clade B SOSIPs	AMC008	B	1B	++	++	++	++
	AMC009	B	2	++	++	++	++
	AMC011	B	2	-	-	+/-	-
	AMC016	B	3	++	++	++	+
	AMC018	B	2	++	++	++	+
	SHIV162p3	B	2	++	+	++	+/-
	REJO	B	2	++	++	++	++
non-clade B SOSIPs	BG505	A	2	-	-	-	-
	ConM	M	1A/1B	-	-	-	-
	CNE55	CRF01_AE	2	-	-	-	-
	BJOX00200 0.03.2	CRF07_BC	2	-	-	-	-
	Ce1176_A3	C	2	++	++	++	-
	HIV_25710- 2.43	C	2	-	-	-	-

^aEnzyme-limited immunosorbent assay (ELISA) cross-binding ability (50% effective concentration [EC₅₀] in $\mu\text{g/ml}$) of the isolated AMC008 SOSIP trimer-reactive neutralizing antibodies (NABs) to various clade B and non-clade-B SOSIP Env trimers. Env trimer binding ability is depicted with colors and symbols, where green colored cells (++) and (+) indicate EC₅₀ higher or equal to AMC008 binding titers, orange (+/-) indicates lower IC₅₀s and red (-) indicates no binding.

07A1 CDRL3 region was similar to that of 05A1-3 (79% sequence similarity). This shared CDRL3 was relatively long, with a length of 14 amino acids. The heavy chain CDR sequences of the 05A family and that of 07A1 did not show any similarities (Fig. 1C).

AMC008 SOSIP-induced NABs cross-neutralize some clade B viruses. The cross-binding ability of the NABs was tested against a panel of 12 heterologous SOSIP Env trimers (Table 1). This panel included four clade B SOSIP Env trimers (AMC009, AMC011, AMC016, and AMC018) based on virus sequences from individuals enrolled in the ACS (34). The Env sequences from these four clade B SOSIP trimers have >83% sequence identity with the AMC008 Env protein. Additional clade B SOSIP Env trimers derived from SHIV162p3 and REJO, showing 79% and 84% sequence identity, respectively, with AMC008, were also included in the panel, as neutralization of these viruses by the corresponding rabbit sera was observed previously (10). Furthermore, we included a selection of non-clade-B SOSIP trimers from a representative global panel, i.e., CNE55 (clade CRF01_AE), BJOX002000.03.2 (clade CRF07_BC), Ce1176_A3 (clade C), and 25710-2.43 (clade C) (35), as well as BG505 (clade A) (5) and, finally, the ConM SOSIP trimer, a consensus sequence protein based on the consensus sequences of each individual HIV-1 group M clade (36). All four NABs displayed cross-reactivity with five out of the six clade B SOSIP Env trimers (Table 1). The NAB family 05A1-A3 also bound to the clade C SOSIP trimer Ce1176_A3, but there was no binding to other SOSIP trimers, suggesting that the target epitope is fairly conserved in clade B isolates but not across different clades.

All four NABs were then tested for neutralization breadth against a panel of 17 heterologous viruses consisting of a subpanel representing the global diversity of HIV-1 supplemented with a number of clade B viruses (35). Two of the viruses in this heterologous panel, the clade B tier 2 viruses SHIV162p3 and AMC009, were cross-neutralized by all four NABs (Table 2). SHIV162p3 was neutralized relatively weakly, with IC₅₀ values ranging from 5.6 to 19 $\mu\text{g/ml}$, i.e., similar to those against the autologous AMC008 virus. Heterologous AMC009 neutralization by the NABs was much weaker, with IC₅₀ values ranging from 58 to 177 $\mu\text{g/ml}$. The relative cross-neutralization of autologous AMC008 and heterologous SHIV162p3 and AMC009 is consistent with the cross-neutralization titers of the sera of rabbits 1605 and 1607 (10).

AMC008 NABs target an epitope on the gp41 subunit. Because the four NABs had nearly identical CDRL3 sequences and three of them were clonal family members, we hypothesized that they might target a shared epitope. To test this, we performed competition assays between these four NABs using biolayer interferometry (BLI). All

TABLE 2 Neutralization ability (IC₅₀ in $\mu\text{g/ml}$) of the autologous NABs to neutralize a panel of 17 heterogeneous viruses.

IC ₅₀ ($\mu\text{g/ml}$)	Clade	Glycan hole	05A1	05A2	05A3	07A1	05D1
AMC008	B	230 + 234	20.5	14	15.1	16.2	>50
SHIV162p3	B	230	8.8	5.6	18	6.1	0.72
AMC009	B	230	177	58	170	114	>200
AMC016	B	-	>200	>200	>200	>200	>200
AMC018	B	234	>200	>200	>200	>200	>200
BaL	B	230 + 234	>200	>200	>200	>200	>200
WITO4160.33	B	234	>200	>200	>200	>200	>200
CH040	B	230 + 234	>200	>200	>200	>200	>200
CZA97.012	C	234	>200	>200	>200	>200	>200
ZM109F	C	234	>200	>200	>200	>200	>200
25710-2.43	C	230	>200	>200	>200	>200	>200
Ce1176_A3	C	-	>200	>200	>200	>200	>200
X2278	B	230	>200	>200	>200	>200	>200
BJOX002000.03.2	CRF07_BC	230	>200	>200	>200	>200	>200
Ce703010217_B6	C	-	>200	>200	>200	>200	>200
X1632-S2-B10	G	230	>200	>200	>200	>200	>200
CNE55	CRF01_AE	230	>200	>200	>200	>200	>200
CH119.10	CRF07_BC	230	>200	>200	>200	>200	>200

NABs showed strong and reciprocal competition with each other, suggesting that their epitopes overlap (Fig. 2A). Differences in percentage of residual binding were observed depending on the directionality of the assay. For instance, we observed 54% residual binding of 05A2 after preincubation with competitor 07A1 MAb. However, only 9% residual binding of 07A1 was measured when 05A2 was used as the competitor. These differences could be due to differences in affinity of the NABs. All MAbs showed self-competition (46 to 27% residual binding) (Fig. 2A).

We then performed competition assays with known human bNABs using ELISA and surface plasmon resonance (SPR) to specify the epitope targeted by these four NABs. We tested competition with bNABs VRC01, PGT121, 35O22, 3BC315, PGT151, and ACS202. These bNABs target diverse regions on the Env trimer enabling us to define a potential binding area of NABs 05A1-A3 and 07A1. All four NABs competed significantly in ELISA with bNABs 35O22, 3BC315, and VRC34, which all target gp41. Competition of the four NABs 05A1, 05A2, 05A3, and 07A1 with 35O22 was weakest, with residual binding being 58%, 69%, 73%, and 67%, respectively (Fig. 2B). The four NABs competed more efficiently with VRC34 and 3BC315, with residual binding between 25% and 60% (Fig. 2B). Weak but not statistically significant competition was observed with gp41-gp120-targeting bNAb ACS202 and no statistically significant competition was detected with gp41-gp120-targeting bNAb PGT151, or bNABs VRC01, or PGT121, which bind to the CD4bs and the V3-N332 glycan epitope, respectively.

SPR analyses strengthened the evidence for competition of the 05A family with gp41-gp120-targeting bNABs 35O22 (~25% residual binding) and ACS202 (~60% residual binding), and also revealed weak competition with PGT151 (~80% residual binding) (Fig. 2B). The competition with ACS202 was enhanced when the SPR assay set-up was reversed. In this reversed set-up, where ACS202 was allowed to bind first and 05A1-3 second, the residual binding dropped to ~10% (Fig. 2C). No significant competition of the rabbit NABs with the bNABs VRC01 and PGT121 was observed in the SPR assays in either set-up (Fig. 2B). These competition results suggest that the AMC008 SOSIP induced NABs that most likely target an epitope at or near the gp41-gp120 interface area.

We also tested competition of the AMC008 SOSIP trimer-induced NABs with the non-NABs elicited against the same immunogen, using BLI. The binding of the four NABs to the AMC008 SOSIP trimers was completely or partially abrogated when any of the five non-NABs 06A1, 07B1, 07D2, 07E1, or 08A1 was present. These competition results suggest that these five non-NABs have overlapping epitopes with the NABs

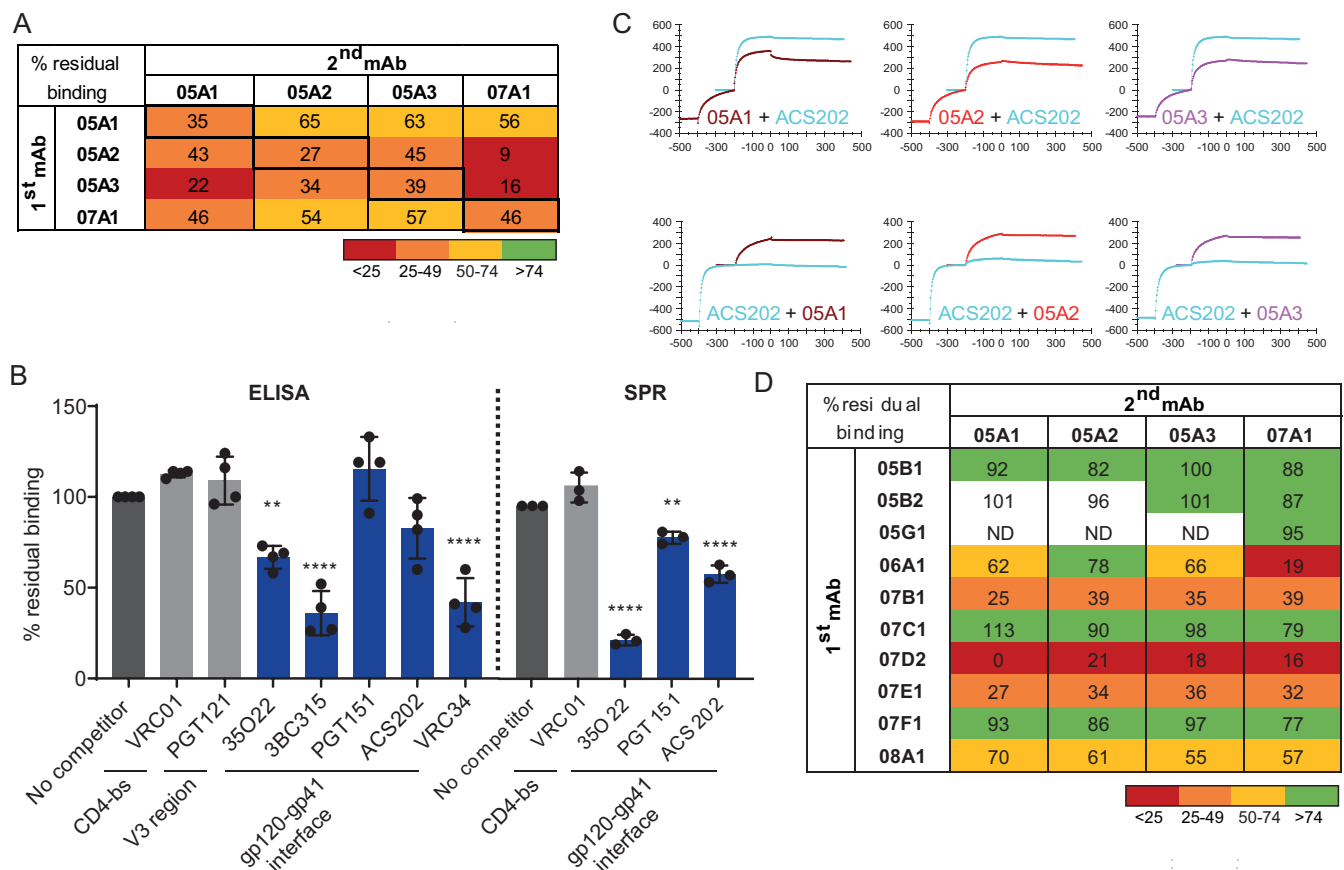


FIG 2 Competitive assays of NABs with bNABs and non-NABs to specify an epitope. (A) Percent residual binding of NABs to AMC008 SOSIP trimers in the presence of a competing NAB. The percent residual binding was calculated as follows: (shift in nm at 600 s of 2nd MAb binding × 100)/(shift in nm of 2nd MAb in the absence of 1st MAb binding). (B) Competition enzyme-limited immunosorbent assay (ELISA) and surface plasmon resonance (SPR) data of all NABs with human broadly neutralizing antibodies (bNABs). The percent residual binding was calculated as follows. For ELISA, (average optical density at 450 nm [OD₄₅₀] of a triplo in the presence of the 2nd MAb × 100)/(average OD₄₅₀ of a triplo in the absence of the 1st MAb binding); for SPR: [(response difference at 200 s for the second Ab)/(response difference at 200 s for the same, second Ab when injected as a single Ab in a separate cycle)] × 100 (%). Significant results are highlighted by asterisks (**, P < 0.005; ***, P < 0.0001). SPR was only performed for the 05A family of NABs. (C) SPR binding curves of AMC008 SOSIP trimer binding competition between NABs and the bNAb ACS202 that shows the influence of assay directionality. Ab binding is recorded in real time; the x axis indicates the time in seconds. The y axis shows the response (response units [RU]), proportional to the mass bound. Dissociation starts at 0 s. The top three graphs show binding of ACS202 in the presence of competitors 05A1 to 05A3 (dark red, red, and purple lines), compared to ACS202 binding in the absence of these NABs (blue lines). The lower three graphs show a reverse assay setup, showing binding ability of NABs 05A1 to 05A3 in the presence of competitor ACS202 (blue lines) and in the absence of ACS202 (dark red, red, and purple lines). (D) Competition results of the four rabbit NABs with the isolated non-NABs, measured by BLI. Percent residual binding was calculated as stated for Fig. 2A.

(Fig. 2D). The remaining five non-NABs did not compete with the NABs, suggesting these target different epitopes on the Env trimer.

Negative-stain electron microscopy (NS-EM) was performed to further delineate the NAB epitope and to confirm its location at or near the gp41-gp120 interface. Binding of Fab fragments from the four identified NABs to the AMC008 SOSIP trimer was visualized through three-dimensional (3D) reconstructions. The NAB Fabs interacted with the gp41 subunit of the AMC008 SOSIP trimer, possibly interacting with residues S528 to A532, N616 to N625, and Q658 to D644 in the HR2 region (Fig. 3A). Additional NS-EM analysis carried out with 05A3 revealed that it bound with a predominant stoichiometry of two Fabs to one Env trimer, although full occupancy of three Fabs binding to one trimer could be detected in a minority of cases. Interestingly, the NABs interacted with the Env trimer with unusual approach angles that would *a priori* be expected to lead to a clash of the NABs with the viral membrane.

AMC008 NABs target residues 620 and 624 in HR2. The NS-EM analysis enabled us to make informed changes to identify amino acid residues important for binding and neutralization. Within predicted interaction regions pinpointed by the NS-EM analysis, we searched for differences between the sequences of Env trimers that the NABs

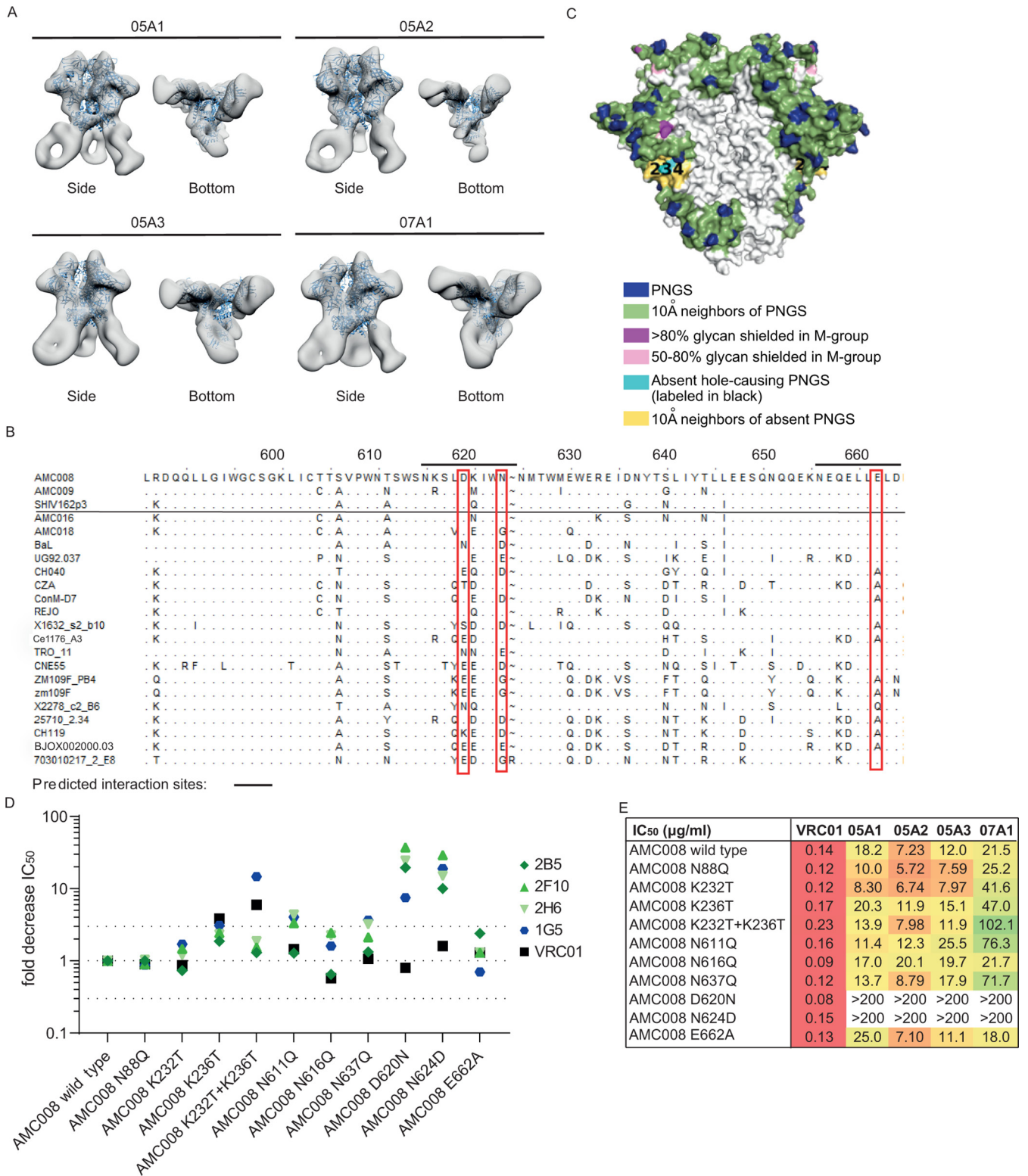


FIG 3 Epitope mapping of NAb to the gp41 subunit of Env. (A) Negative-stain electron microscopy (NS-EM) 3D reconstructions of the NAb Fab fragments in complex with the AMC008 SOSIP trimer. The AMC008 SOSIP trimer structure is modeled as the ribboned density. The NAb is shown as white densities. Side and bottom views are depicted. (B) Alignment of viral sequences tested for neutralization and binding by 05A1 to 05A3 and 07A1. AMC008, AMC009, and SHIV162p3 could be neutralized by the NAb, whereas the viruses below the line were not neutralized by the NAb. HXB2 amino acid numbering is indicated on top, and lines indicate the NAb binding sites predicted by NS-EM imaging. Red boxes show which amino acid residues were mutated in the predicted binding sites to specify the epitope, namely, D620N, N624D, and E662A. (C) Model of the glycan shield present on the AMC008 SOSIP trimer with a strain-specific glycan hole indicated in cyan and yellow due to the absence of PNGS 230 and 234. Image was created with the glycan

(Continued on next page)

were able to cross-bind and/or neutralize and those of trimers that they could not bind or neutralize (Fig. 3B). Divergent amino acids were mutated in the context of the AMC008 SOSIP trimer and the corresponding pseudovirus to the most prevalent amino acid in the nonbinding sequences, resulting in three variants with single amino acid substitutions, i.e., D620N, N624D, and E662A. In addition, considering that Env glycans might influence NAb binding, we modified the glycan shield near or on gp41 of the AMC008 trimer. Accordingly, knockout (KO) mutants of the potential *N*-linked glycosylation sites (PNGS) at positions 88, 611, 616, and 637 were created. Finally, since previous studies showed that SOSIP-induced NAb often target strain-specific holes in the glycan shield (15–17, 25), we knocked in the PNGS at positions 230 and 234 of the AMC008 sequence, as the absence of PNGS at these positions in the natural AMC008 sequence is expected to create a strain-specific glycan hole (Fig. 3C). Substitution of amino acids 620 and 624 abolished neutralization ability of all four NAb, but not of the control Ab VRC01, consistent with the NS-EM data (Fig. 3D and E). Furthermore, neutralization by 07A1 was also affected by simultaneously introducing the N230 and N234 PNGS, although these substitutions did not completely abrogate activity, as neutralization of the virus still occurred at higher Ab concentrations. This suggests that glycans at N230 and N234 restrict access to the 07A1 epitope. Three out of four NAb were also affected by removing the N611 and N637 PNGS; these glycans might therefore contribute to (the presentation of) the NAb epitope. The K232T and K236T single-knock-in (KI) mutations did not affect neutralization for any of the four NAb, nor did the N88 and N616 KO mutations or the E662A amino acid substitution. When residues 230, 234, 611, 620, 624, or 637 were mutated in the AMC008 SOSIP trimer context, it did not detectably affect binding of NAb 05A1 to 05A3 in ELISA, while the effect on NAb 07A1 was only observed when residues 620 and 624 were changed (Fig. 4A). Differential effects of single mutations in neutralization versus binding assays have been observed in other cases (37, 38), and these probably relate to affinity and Env protein conformation and stability.

We were also able to define the epitopes for the majority of the non-NAb. MAb 07E1 and 07D2 also showed dependence on the 620, 624, and/or 662 amino acids in ELISA (Fig. 4A), confirming their epitope overlap with the NAb, as suggested by the competition experiments. NS-EM further confirmed this epitope overlap for non-NAb 07D2 (Fig. 4B). Other non-NAb bound a variety of epitopes on the gp41 subunit of the Env trimer, such as the area around the N637 glycan (07F1) (Fig. 4A) and an epitope at the base of the Env trimer (07B1). The non-NAb 05D1 was able to bind a linear V3 peptide in ELISA (Fig. 4A).

NAb and non-NAb targeting the 620/624 site cannot be differentiated based on affinity for soluble trimers. We were intrigued by the identification of NAb and non-NAb that targeted overlapping epitopes. A first hypothesis would be that binding affinity might explain the differences in neutralization ability between NAb and non-NAb. To test this, we subjected a subset of AMC008 SOSIP-induced non-NAb and all four NAb to kinetic binding experiments with AMC008 SOSIP Env trimers. No significant differences were observed in affinity between the NAb and the non-NAb ($P=0.057$ for K_D [equilibrium dissociation constant], $P=0.057$ for K_a [association constant], and $P>0.999$ for K_d [dissociation constant]; Mann-Whitney U test) (Fig. 5A).

We also noted that all four NAb were able to cross-bind certain SOSIP Env trimers, but were unable to neutralize their corresponding virus. We asked whether this observation could be explained by differences in affinity as well. We tested all four of the NAb in kinetic binding experiments using AMC008 SOSIP and AMC016 SOSIP Env trimers. The latter was selected in addition to the autologous trimer because the AMC016 virus

FIG 3 Legend (Continued)

shield mapping tool on the Los Alamos database (57). (D) Neutralization ability of NAb to multiple viral variants. Fold decrease in IC_{50} values is plotted for each of the NAb and the VRC01 control, each represented by different colors. The dotted lines indicate a 3-fold threshold compared to AMC008 wild-type neutralization IC_{50} values. (E) Neutralization ability of the NAb for various AMC008 mutants. IC_{50} values are indicated in $\mu g/ml$. The bNAb VRC01 is taken along as a positive control.

A

Ab ID	Fold change AUC												linear V3 peptide
	AMC008 v4.2	AMC008 gp120	K232T	K236T	K232T+K236T	N88Q	N611Q	N616Q	N637Q	D620N	N624D	E662A	
2G12	1.0	1.0	0.9	0.9	0.9	0.8	0.8	0.9	0.9	0.9	0.8	0.9	No
PGT145	1.0	ND	1.0	1.0	0.9	0.8	0.8	0.9	0.8	1.5	0.9	1.1	ND
05A1	1.0	0.1	0.8	0.7	0.7	0.8	0.8	0.8	0.9	0.7	0.6	0.8	No
05A2	1.0	0.1	0.9	0.9	0.9	0.3	0.8	0.9	0.9	0.9	1.0	1.0	No
05A3	1.0	0.1	0.9	0.9	1.0	0.9	1.0	1.0	0.9	1.0	0.8	0.9	No
05B1	1.0	ND	ND	ND	ND	ND	ND	ND	ND	1.0	1.0	1.0	ND
05B2	1.0	0.1	0.9	0.9	0.9	0.9	1.1	1.0	1.7	0.7	0.8	1.1	No
05D1	1.0	0.1	0.9	0.8	1.0	0.8	0.5	0.8	0.8	0.8	0.7	0.9	Yes
05G1	1.0	0.0	0.9	0.9	0.9	0.9	0.8	0.9	0.7	0.6	0.4	0.9	ND
06A1	1.0	0.0	0.8	0.8	0.8	0.9	0.5	0.8	1.0	1.0	0.8	1.0	ND
07A1	1.0	0.0	0.9	0.9	0.9	0.9	0.9	0.9	0.9	0.1	0.6	1.0	ND
07B1	1.0	1.4	1.0	1.0	1.0	1.0	1.0	1.1	1.0	0.9	1.0	1.2	No
07C1	1.0	0.1	1.0	0.9	1.0	0.9	1.1	1.1	1.1	0.7	0.9	1.1	No
07D1	1.0	ND	ND	ND	ND	ND	ND	ND	ND	ND	ND	ND	ND
07D2	1.0	0.0	1.0	0.7	0.7	0.7	0.6	1.2	1.2	0.1	0.1	0.1	ND
07E1	1.0	0.1	1.2	0.8	1.0	0.8	1.4	1.7	0.9	0.8	0.4	0.6	ND
07F1	1.0	0.1	1.0	1.0	0.8	0.9	1.0	1.0	0.3	0.9	0.9	0.9	No
07G1	1.0	ND	ND	ND	ND	ND	ND	ND	ND	ND	ND	ND	ND
08A1	1.0	ND	0.9	1.0	1.0	0.9	0.7	0.9	0.7	1.0	0.8	0.9	ND
			Strain specific glycan hole			gp41 glycans				NAb Interaction site			V3

0.1-0.3

0.4-0.6

0.7-1.0

>1.0



FIG 4 Epitope mapping of the nonneutralizing antibodies. (A) Binding ability of all isolated MABs to various AMC008 mutants and linear V3 peptide. Fold change in area under the curve is displayed relative to AMC008 binding. Binding to the V3 peptide is indicated as “yes” or “no.” (B) NABs 05A1 to 05A3 (purple and pink) and 07D2 (gray) were complexed with the AMC008 SOSIP Env and analyzed by NS-EM with the AMC008 SOSIP trimer to show differences in their binding angle.

was not neutralized by our NABs, while they were able to bind to the corresponding AMC016 SOSIP trimer (Table 2). AMC016 SOSIP trimers contain the amino acids essential for neutralization (D620 and N624), but also the N230 and N234 PNGS that are absent from the AMC008 Env sequence. Kinetic analysis did not reveal significant differences in NAb binding kinetics between the AMC008 SOSIP and AMC016 Env trimers ($P=0.343$ for K_{Dr} , $P=0.114$ for K_{Dr} , and $P=0.486$ for K_{Dr} ; Mann-Whitney U test) (Fig. 5A), suggesting that binding kinetics are not the main cause for the (in)ability of these NABs to neutralize these viruses.

NABs and non-NABs targeting the 620/624 site cannot be differentiated based on binding to membrane-associated Env trimers. The next hypothesis posits that the discrepancy between binding and neutralization ability of the autologous AMC008 SOSIP Env trimer-reactive MABs might be due to an inability of the non-NABs to bind full-length surface-displayed Env trimers, possibly related to the observed unusual approach angle. To test this, we transfected HEK293 cells with AMC008 SOSIP gp160 Env constructs (39), which resulted in surface-expressed AMC008 SOSIP trimers that were subsequently analyzed by FACS to detect MAB binding (Fig. 5B). In contrast to what we expected, we found that NABs and non-NABs bound similarly to full-length cell surface-displayed AMC008 SOSIP gp160 trimers. Surprisingly, we found that the NAB 05A3 bound weakly, and NAB 07A1 was unable to bind cell surface-displayed SOSIP gp160 trimers, which is somewhat inconsistent with their ability to neutralize.

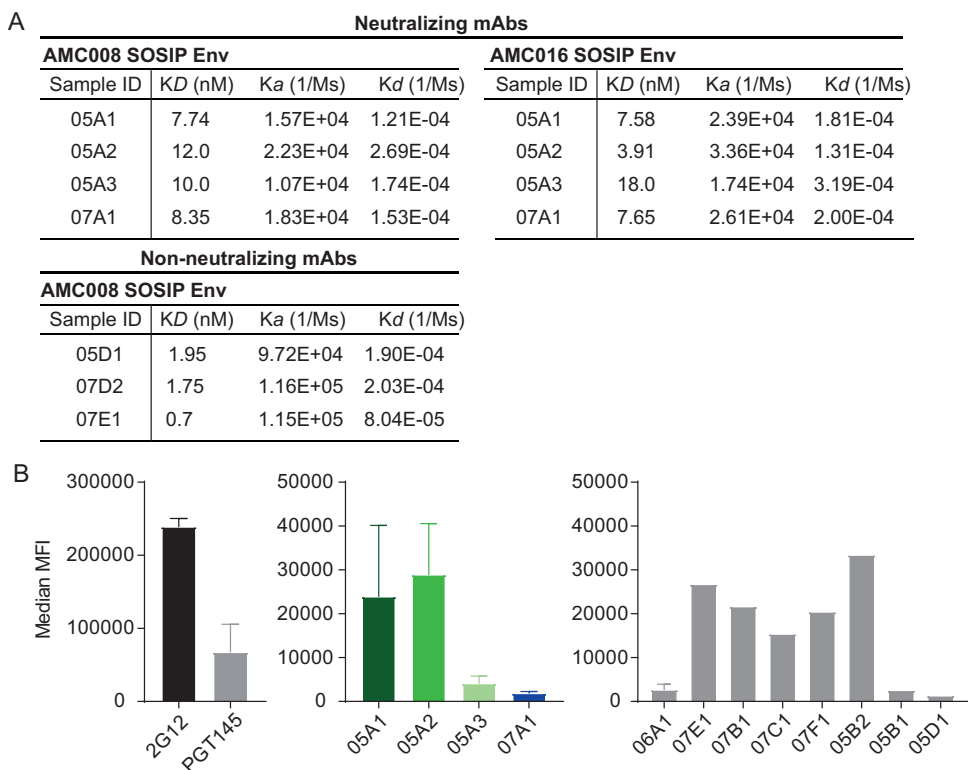


FIG 5 Analysis of neutralizing and nonneutralizing antibody characteristics that might influence neutralization. (A) Binding kinetics of NAb and non-NAb to the autologous AMC008 SOSIP and heterologous AMC016 SOSIP Env trimers. K_D , on-rate (K_a), and off-rate (K_d) constants are shown. NAb was tested for binding to AMC008 and AMC016 SOSIP Env trimers. Non-NAb was only tested for binding to the autologous AMC008 SOSIP trimer. Results were fitted to a 1:1 kinetics model for analysis. (B) Binding to full-length surface-expressed AMC008 SOSIP gp160 Env by MAb. Maximum mean fluorescent intensity (MFI) is plotted for each MAb tested. (Left) Binding and expression controls (2G12 and PGT145, respectively). (Middle) Binding of the NAb to full-length AMC008 gp160 Env trimers. (Right) Binding of a selection of non-NAb to full-length AMC008 gp160 Env trimers.

Neutralization activity of MAb against the 620/624 epitope is determined by their ability to disrupt the trimer. A third hypothesis argues that the strength of neutralization is strongly influenced by the capability to induce trimer dissociation. Indeed, gp41 targeting human bNAb 3BC315 and 3BC176 neutralize by inducing dissociation of the Env trimer, and so does rabbit bNAb 1C2 derived from an immunization study (1, 29). We noticed that the 05A3 Fab fragments caused the trimer to dissociate into monomers during sample preparation for NS-EM (Fig. 6A). Dissociation of the AMC008 SOSIP Env trimer did not occur spontaneously when the trimer was left overnight at room temperature in the absence of 05A1 or 05A3, suggesting that the Fab was responsible for the observed trimer dissociation.

To corroborate these findings, we performed a neutralization assay with prolonged preincubation times (29). This assay determines the neutralization ability of an Ab after preincubation over a 24-h time period at 37°C to measure irreversible trimer destabilization. An increase of neutralization with longer incubation times is indicative of trimer destabilization, as more trimers are destabilized by the Ab over time (1, 29). The bNAb PGT126 and 3BC315 were tested in this assay as negative and positive controls, respectively, and showed an increase in neutralization potency of 1.5-fold and 10-fold, respectively, after 24 versus 1 h of incubation. The potency of our NAb against the autologous AMC008 virus increased by ~10-fold after 24 h of incubation (Fig. 6B), indicative of trimer dissociation and similar to the effect of 3BC315. The non-NAb 6A1, targeting a similar epitope as our NAb, remained unable to neutralize the AMC008 virus even after 24 h of incubation. The results were even more pronounced with the heterologous SHIV162p3 virus, showing increases in potency of up to nearly 30-fold after 24 h. Interestingly, NAb 05A1 did show

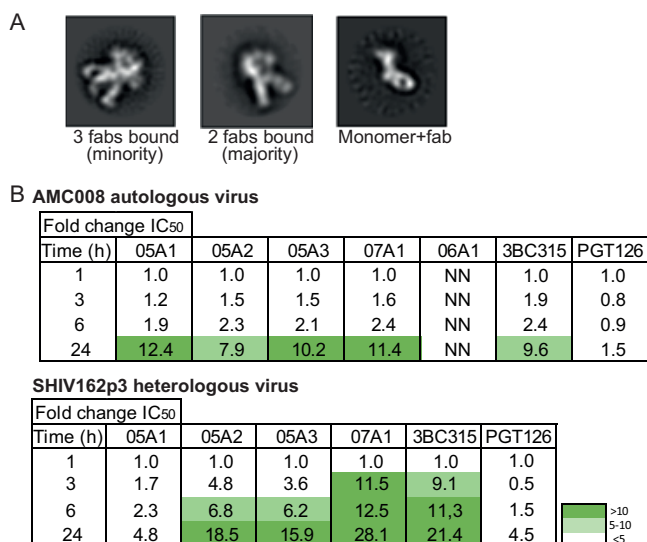


FIG 6 NAbs destabilize the trimer as a mechanism of neutralization. (A) Negative-stain electron microscopy images of AMC008 SOSIP trimers incubated overnight with the MAb 05A3. The majority of the images displayed MAb binding with a stoichiometry of 2 MAbs per trimer (middle). MAbs binding the monomeric form of the trimer were also observed (right). (B) Preincubation neutralization experiment to determine the *in vivo* destabilization ability of the isolated Abs. A neutralization assay was performed in which virus and Ab mix were incubated for different time periods, up to 24 h. The fold change in IC₅₀ is shown for each of the Abs. The autologous AMC008 virus and heterologous SHIV162p3 viruses were tested. 3BC315 and PGT126 were tested as positive-control and negative-control Abs, respectively. Increased neutralization potency after the 24-h incubation step is seen for most of the NABs and for 3BC315, but not for 06A1 and PGT126. NN, nonneutralizing.

an increase in potency against the AMC008 virus over time, but no significant increase against the heterologous SHIV162p3 virus. Nevertheless, these data indicate that the four NABs dissociate Env trimers of both autologous and heterologous viruses and that this largely contributes to their neutralization capacity.

DISCUSSION

To overcome viral diversity, an HIV-1 vaccine should induce bNAbs. However, the currently used immunogens have been unable to consistently elicit such responses. In this study, we tried to better understand the humoral immune responses after HIV-1 SOSIP Env trimer immunization in rabbits. We set out to determine which epitopes on the clade B AMC008 SOSIP Env trimer were targeted and whether the observed specificities could explain the low-titer heterologous neutralization that was observed after immunization with this SOSIP trimer. We isolated and characterized 17 MAbs from four AMC008 SOSIP Env trimer-immunized rabbits. The vast majority of the isolated MAbs targeted a similar area in the HR2 region. One Ab family (05A) and the MAb 07A1 were found to neutralize the autologous and two heterologous viruses through destabilization of the Env trimer, a mechanism of neutralization also used by NABs induced by natural infection or vaccination (1, 29). Additionally, we identified important contact residues for these NABs. Such knowledge may help to shape next-generation SOSIP Env trimer immunogens to induce trimer-destabilizing NABs.

Even though rabbits are a widely used animal model in the early stages of HIV-1 vaccine testing, we realize there are caveats to using this model. In contrast to humans, rabbits interact with the antigen predominantly through their light chain (32) and use one heavy V-gene in the initial Ab recombination process; therefore, diversity in the heavy chain is much more restricted compared to that in their light chains. Additionally, gene conversion and somatic hypermutation (SHM) are the major drivers of Ab diversity in rabbits; the former is a process that rarely takes place in humans (32, 40). Nonetheless, numerous isolated rabbit Abs show that similar epitopes on the Env trimer are targeted compared to those seen in macaques and humans after natural infection (15).

Although the NABs that we describe do not have the desired breadth for a protective HIV-1 vaccine, they are rare examples of MAbs with consistent, albeit weak, cross-neutralizing ability, in particular after only three immunizations with only one immunogen. Other experiments have yielded only autologous neutralizing MAbs, with the notable exception of the isolation of two bNAbs from one Env-immunized rabbit (1, 16, 19, 25). Valuable information from these previous studies led to the development of new immunogens, such as Env trimers displayed on nanoparticles, germ line trimers, and specific epitope scaffolds that were expected to induce more broad and consistent neutralization (2, 27, 41, 42). Nonetheless, neutralization breadth in rabbits after HIV-1 immunization remains sporadic and is usually of low titer (9–12). The isolation of heterologous NABs from multiple rabbits using the same neutralization mechanism and targeting similar epitopes highlights the possibility for immune focusing toward this epitope cluster. The identification of bNAbs isolated from both humans and rabbits that target similar epitopes, with the shared capacity to disrupt trimers, marks this epitope as a very interesting target to be further exploited (1, 29).

bNAb 1C2, which exhibited an extraordinary broad NAb response (~85%) was isolated from an Env-immunized rabbit (1). The mechanism of 1C2 neutralization involved destabilization of the Env trimer, similar to the effects of bNAbs 3BC315 and 3BC176 (29) and NAb family 05A and 07A1 described here. It was proposed that these bNAbs destabilize the trimer by disruption of the stabilizing tryptophan clasp formed by amino acids W623, W628, and W631 (1, 43). The CDRH3 loops of both rabbit bNAb 1C2 and human bNAb 3BC315 are close to residue W623 of this clasp. Because the NABs we describe here have contacts with residues 620 and 624, neighboring this tryptophan clasp, it is not unlikely that a similar disruption mechanism is utilized by these rabbit NABs. The description of multiple (b)NABs directed to this epitope, with the same potent mechanism of action, indicate this epitope as a potential vaccine target. Nonetheless, the isolation of bNAbs, NABs, and non-NABs directed to this epitope shows that adaptations to the immunogen are necessary to amplify this desirable response and guide the responses to neutralization potency and breadth. One strategy involves glycan modifications to enhance accessibility of the tryptophan clasp. Another complementary strategy could involve immune focusing on conserved amino acids within this region, as opposed to ones that are more variable, such as residues 620 and 624.

The AMCO08 SOSIP Env trimer lacks the N230 and N234 PNGS, generating a strain-specific glycan hole. The absence of these glycans might dictate the angle of approach for the NABs identified in this study and thereby restrict the breadth of the response. Filling the 230/234 glycan hole negatively impacted neutralization by the NAb 07A1. However, this was not the case for the NABs isolated from animal 1605. One explanation might be that the footprint of the 07A1 epitope is larger and/or in closer proximity to the 230/234 glycan hole. The ability of these NABs to neutralize viruses containing the 230 and 234 PNGS, such as the SHIV162p3 virus, is encouraging, as the 234 PNGS is widely conserved.

The NS-EM revealed an improbable approach angle for the NABs that should result in a clash with the viral membrane. It is possible that the angles by which the NABs approach soluble Env trimers and virus-associated Env might differ, in particular at the trimer stem. For instance, the membrane-proximal external region (MPER) bNAb 10E8 Fab approaches soluble SOSIP trimers with an angle similar to that of 05A1 to 05A3 and 07A1, but this angle changes to facilitate the presence of the membrane when 10E8 binds to membrane-anchored Env (44). Moreover, viral membrane-associated envelope proteins can have remarkable flexibility. This flexibility was visualized for the severe acute respiratory syndrome coronavirus 2 (SARS-CoV-2) spike protein, which is able to tilt by up to ~60° relative to a position perpendicular to the membrane (45). Also, HIV-1 Env trimers on nanodiscs displayed the ability to tilt by ~20° when bound to gp41-directed bNAbs (28).

Previous studies suggested that a lower rate of dissociation was associated with stronger neutralization (21, 22). However, this did not apply to the gp41-directed MAbs described here. One difference is that these MAbs originated from different clonal families, whereas

the previous studies analyzed members from the same family. Furthermore, we determined binding kinetics using stabilized soluble Env SOSIP trimers. The possibility cannot be excluded that Env stabilization in the SOSIP construct and the observed destabilization of the Env trimer by the Nabs might have affected the affinities we measured. Nevertheless, it is likely that a low dissociation rate and the ability to induce trimer dissociation are distinct properties that affect both neutralization potency and efficacy (46).

In summary, characterizing humoral immune responses at the MAb level after immunization can inform future immunization studies and strategies. We found that gp41-directed NAbs with an unusual approach angle that was predicted to clash with the viral membrane were able to weakly neutralize autologous and heterologous clade B viruses by inducing Env trimer destabilization, reminiscent of bNAbs that induce trimer dissociation by disrupting the tryptophan clasp in gp41. This knowledge highlights that destabilization of the trimer might be a more important neutralization mechanism than previously appreciated. Inducing trimer-destabilizing NAbs that target the tryptophan clasp should be considered in future immunization strategies.

MATERIALS AND METHODS

Isolation of rabbit peripheral blood mononuclear cells. Blood of immunized rabbits was used for peripheral blood mononuclear cell (PBMC) isolation through Ficoll separation. In short, blood was diluted 1:1 with phosphate-buffered saline (PBS), loaded on a Ficoll layer, and centrifuged for 30 min at room temperature at $400 \times g$ with an acceleration speed of 7 and a deceleration speed of 0. PBMCs were isolated, washed with PBS, and subsequently resuspended in 1 to 2 ml of ammonium-chloride-potassium (ACK) buffer (Thermo Fisher Scientific) to remove red blood cells. PBMCs were counted, suspended in fetal calf serum with 10% dimethyl sulfoxide (DMSO), and directly frozen at -150°C .

Env protein design, production, and purification. All SOSIP trimers contained the previously described SOSIP mutations (8) and were further stabilized with additional mutations, yielding SOSIP.v4.2 (E66K + A316W) trimers (10). ConM and SHIVp3 SOSIP trimers contained additional mutations (SOSIP.v9), described elsewhere (47–49). All SOSIP constructs were cloned into a pPPI4 expression vector (50). Mutant variants were generated by the use of the Q5 site-directed mutagenesis kit (New England Biolabs) with specifically designed primer sets and adapted annealing temperatures for the mutations N88Q, K232T, K236T, K232T+K236T, N611Q, N616Q, N637Q, D602N, N624D, and E662A. D7324 tags were incorporated directly C-terminal of residue 664 in each of the plasmids (8). In addition, we replaced the D7324 tag C-terminal of residue 664 with an Avi tag in the AMC008 SOSIP.v4.2 construct for biotinylation (16). For BLI and SPR experiments an His tag was incorporated into AMC008 SOSIP.v4.2 and the AMC008 SOSIP.v4.2 D620N, N624D, and E662A mutant plasmids, replacing the D7324 tag (2).

All SOSIP trimer variants were produced as described before (6, 8, 10, 51, 52). In short, SOSIP trimers were transiently expressed together with furin from a separate expression plasmid (ratio, 4:1) in HEK293F cells (catalog no. R79009; Invitrogen). The SOSIP trimers were harvested by spinning for 20 min at $4,000 \times g$. The supernatant was $0.22 \mu\text{M}$ Steritop vacuum filtered before purification by gravity-driven chromatography on a PGT145 antibody-conjugated Sepharose column. Env proteins were eluted with 3 M Mg_2Cl_2 (pH 7.8), directly into neutralization buffer (20 mM Tris-HCl [pH 8.0] and 75 mM NaCl). After purification, Env proteins were concentrated with Vivaspin 100-kDa filters (GE Healthcare), to a final volume of $<500 \mu\text{l}$. AMC008 SOSIP.v4.2-Avi was biotinylated to allow conjugation for FACS analysis. BirA biotin protein ligase (Avidity) was used for the biotinylation.

Antibody production and purification. HEK293F cells (catalog no. R79009; Invitrogen) were transfected to produce MAbs as described previously (16). In short, $62.5 \mu\text{g}$ of each heavy and light chain Ab DNA were cotransfected transiently in 250 ml HEK293F cells. Cell supernatant was harvested at 5 days by spinning down for 20 min at $4,000 \times g$ and subsequent vacuum filtration with a $0.22\text{-}\mu\text{m}$ Steritop filter. Abs were purified from the culture supernatant by gravity-driven chromatography on a Protein G affinity column (Thermo Fisher Scientific). After addition of the supernatant, columns were washed twice with PBS before elution with 9 ml 0.1 M glycine (pH 2.0). Eluted Abs were collected in 1 ml 1 M Tris-HCl (pH 7.8). After elution, Abs were concentrated, by the use of 100-kDa Vivaspin filters (GE Healthcare) filters, to a final volume of $<200 \mu\text{l}$.

We named the isolated MAbs following McCoy et al. (16). In this system, each MAb is numbered according to their rabbit ID, followed by a unique alphabetical lineage identifier (A, B, C, etc.). Distinct lineage members received an additional number (A1, A2, A3, etc.).

Single B-cell sorting. Single B cells were selected and sorted as previously described (16). Briefly, biotinylated AMC008 SOSIP.v4.2-Avi Env proteins were conjugated to streptavidin (Strep)-allophycocyanin (APC) and Strep-fluorescein isothiocyanate (FITC) (both Thermo Fisher Scientific). Mouse-anti-rabbit IgG Ab conjugated to phycoerythrin (PE)-stained IgG on memory B cells (Southern Biotech). Conjugated Env protein was mixed with PBMCs to allow binding. We first selected IgG-positive (IgG^+) cells and, within this population, sorted single B cells, positive for both APC- and FITC-conjugated AMC008.v4.2 Env trimer, into a lysis buffer consisting of RNase inhibitor (20 U; Thermo Fisher Scientific), $5 \times$ first-strand SuperScript III buffer (Invitrogen), 0.1 M dithiothreitol (DTT; Invitrogen), and Milli-Q water [MQ]. Sorted cells were immediately frozen at -80°C .

Single-cell Ab RT-PCR, variable region gene amplification, and cloning. A 6- μ l aliquot of reverse transcription-PCR (RT-PCR) mixture (200 ng random hex primers [Thermo Fisher Scientific], 2 mM each dNTP mix [New England Biolabs], 50 U SuperScript III RTase, and MQ) was added directly to the sorted single B cells. The following PCR program was used to convert RNA into cDNA: 42°C for 10 min, 25°C for 10 min, 50°C for 60 min, and 95°C for 5 min. RT-PCR plates were used directly for variable region gene amplification using two subsequent PCRs. For both PCRs, 13 μ l of PCR mix (MQ, 10 \times PCR buffer, dNTPs [10 mM], 0.25 U HotStar Plus polymerase [Qiagen], forward primer [25 mM], and reverse primer [25 mM]) was added subsequently to the RT-PCR plate and the PCR 1 plate. For PCR 1, 2 μ l of RT-PCR product was added to this mix. PCR 1 was run at 95°C for 5 min; followed by 50 cycles of 94°C for 30 s, 58°C for 30 sec, and 72°C for 1 min; followed by 72°C for 10 min. For the heavy chain amplification, the annealing temperature was adapted to 48°C. For PCR 2, 2 μ l of PCR 1 product was added to the PCR mix, and DNA was amplified at 95°C for 5 min; followed by 50 cycles of 94°C for 30 sec, 55°C for 30 sec, and 72°C for 1 min; followed by 72°C for 10 min. A final PCR 3 reaction using 1 μ l of PCR 2 product was performed in MQ, 5 \times Phusion PCR buffer, dNTPs (10 mM), forward primers (25 mM), reverse primers (25 mM), and 0.2 U Phusion high-fidelity polymerase (New England Biolabs). The following PCR program was run: 98°C for 30 s; followed by 35 cycles of 98°C for 5 s, 68°C for 15 s, and 72°C for 20 s; followed by 72°C for 5 min.

Heavy and light chain-amplified variable regions were cloned by Gibson cloning into vectors expressing, respectively, the heavy or light chain constant region of rabbit Abs =. In short, 1 μ l vector (45 ng) was incubated with 1 μ l PCR 3 product and 2 \times Gibson mix (0.2 U T5 exonuclease [Epibio], 12.5 U Phusion polymerase [New England Biolabs], 2,000 U *Taq* DNA ligase [New England Biolabs], and Gibson reaction buffer [0.5 g PEG-8000 (Sigma Life Sciences), 1 M Tris/HCl (pH 7.5), 1 M MgCl₂, 1 M DTT, 100 mM dNTPs, 50 mM NAD (New England Biolabs), and MQ]) for 60 min at 50°C.

Mutant virus construction and production. The infectious molecular clone (IMC) encoding replication-competent virus with AMC008 Env has been described previously (10). First, the AMC008 *env* fragment was transferred to pUC18 by traditional cloning methods using restriction enzymes *Sall* and *Bam*HI (New England Biolabs). Mutations were then generated using the Q5 mutagenesis kit (New England Biolabs). Mutated AMC008 *env* fragments were cloned back into the original IMC by Gibson reactions. To produce virus stocks, HEK293T cells (CRL-11268; ATCC) were transfected with the IMCs using Lipofectamine 2000 (Invitrogen) and supernatants containing viruses were harvested 3 days later. Supernatants were directly frozen at -80°C.

Neutralization assays. Neutralization assays were executed as described previously (8, 15). In short, 1 in 3 dilution series were made of the various MAbs, starting at end concentrations ranging from 50 μ g/ml to 100 μ g/ml. Virus of interest was added to the diluted MAb and incubated for 1 h at room temperature. After incubation, the mixture was added to TZM-bl reporter cells (obtained through the NIH AIDS Reagent Program, Division of AIDS, NIAID, NIH, from John C. Kappes and Xiaoyun Wu) and incubated for 3 days at 37°C. IC₅₀ values were determined as the concentration at which infectivity was inhibited by 50%.

For the decay neutralization assays, virus and MAb mixtures were incubated for 1, 3, 6, and 24 h at 37°C before addition to the TZM-bl reporter cells.

Negative-stain electron microscopy. Complex formation was performed by incubating AMC008 SOSIP.v4.2 trimers with a 6-fold molar excess of Fab for 3 h at room temperature. Complexes were subsequently diluted to 0.03 mg/ml in 1 \times Tris-buffered saline (TBS; pH 7.4) to achieve optimal particle density. Copper mesh grids were plasma cleaned for 20 s using a mix of argon and oxygen gas, and samples were stained with 2% uranyl formate for 50 s. For each data set, a FEI Tecnai Spirit (120 keV) with a Tietz (4k \times 4k) camera was used in conjunction with the automated data collection software package Legikon (53). Data collection parameters included a magnification of \times 56,000, a defocus of -1.5 μ m, a pixel size of 2.05 Å per pixel, and a dose of 25 e⁻/Å². Resulting images were stored in Appion (54); particles were picked with DoGPicker (55), stacked with a box size of 192 pixels, and processed using RELION (56). UCSF Chimera (57) was used for map segmentation and map/model docking.

Binding and competition ELISAs. Binding ELISAs were performed as previously described (2, 4). In short, ELISA plates were coated overnight with 100 μ g *Galanthus nivalis* lectin (GNL) in 0.1 M NaHCO₃ (pH 8.6) and blocked using casein (Thermo Fisher Scientific) at room temperature for 1 h after washing off the GNL with Tris-buffered saline (TBS). Env trimers were added at 2 μ g/ml and incubated at room temperature for 2 h. Subsequently, Ab 3-fold serial dilutions were added for 2 h at room temperature at starting concentrations ranging from 1 μ g/ml to 10 μ g/ml. After washing with TBS, a 1:3,000 dilution of goat-anti-human or goat-anti-rabbit horseradish peroxidase (HRP, 1 μ g/ml; SeraCare)-conjugated Ab was added and incubated at room temperature for 1 h. After washing with TBS plus 0.05% Tween 20, ELISA plates were developed using 1% 3,3',5,5'-tetranethylbenzidine (Sigma-Aldrich), 0.01% H₂O₂, 100 mM sodium acetate, and 100 mM citric acid, and reactions were stopped after 3 min using 0.8 M H₂SO₄.

For HEK293T supernatant ELISAs, the same protocol was followed; however, 50 μ l of HEK293T supernatant containing unpurified MAB was added instead of purified Abs.

For competition ELISA, His-tagged Env trimers were added at 2 μ g/ml to pre-coated Ni-nitritriacetic acid (NTA) plates (Qiagen) and left at room temperature for 2 h. Blocking was achieved in 2% milk in TBS at room temperature for 1 h. The primary Ab (competitor) was added at excess (10 μ g/ml) in 50 μ l and incubated for 30 min at room temperature before the analyte Ab was added at a previously determined 70% effective concentration (EC₇₀) in 50 μ l and left at room temperature for another 1.5 h. Statistical significance was determined using a one-way analysis of variance (ANOVA) multiple-comparison test (Prism) comparing the sample without competitor to the corresponding sample with competitor present.

Octet K2 biolayer interferometry kinetics and binding experiments. All assays were conducted on the Octet K2 system (Bioforte). His-tagged AMC008 SOSIP.v4.2-His Env trimer (6 μ g/ml) was captured on Ni-NTA sensors (Bioforte) for 600 s after baseline determination in PBS with 0.01% bovine serum

albumin (BSA) and 0.002% Tween for 60 s. Association of a serial dilution of rabbit MABs starting at 15 $\mu\text{g/ml}$ was measured for 600 s by dipping the AMC008 SOSIP.v4.2 trimer-loaded sensor into a well containing MAB. Subsequently dissociation was measured in buffer (PBS, 0.01% BSA, and 0.002% Tween) for 600 s. Binding kinetics (K_D , K_{on} , and K_{off}) were determined using a 1:1 fit model with independent fitting of R_{max} (Octet Data analysis software; Bioforte). Regeneration of the sensors was achieved through alternating cycles of 5 s in low-pH glycine buffer and a neutralization buffer (PBS, 0.01% BSA, and 0.002% Tween). After regeneration, sensors were used to recapture Env protein.

For competition analysis, after association of the competitor MAB to the SOSIP trimer bound to Ni-NTA sensors, a second 600-s association step was incorporated for the analyte MAB. Percent residual binding was calculated as follows: (shift in nm at 600 s of analyte binding \times 100)/shift in nm of analyte in the absence of competitor binding.

Surface plasmon resonance. Surface plasmon resonance (SPR) experiments were done for kinetic and competition analysis of rabbit MABs, as previously described (34). All assays were conducted on a Biacore 3000 instrument at 25°C. In all assays, HBS-EP (10 mM HEPES [pH 7.4], 150 mM NaCl, 3 mM EDTA, and 0.002% P20 surfactant) was used as running buffer (GE Healthcare). Briefly, anti-His Ab was covalently immobilized (15,000 response units [RU]) in all flow cells of a CM5 sensor chip by standard amine coupling. AMC008 SOSIP.v4.2-His Env trimer was captured on the anti-His-CM5 surface for both kinetic and competition analysis.

Competition assays were carried out with MABs binding to the CD4bs (VRC01), gp120 V3-glycan (PGT121), and the gp120-gp140 interface (PGT151, 35O22, and ACS202). In the competition assays, MABs were sequentially injected in the same cycle. The first Ab was injected for 200 s, immediately followed by the second Ab, at a flow rate of 30 $\mu\text{l/min}$. Dissociation followed for 300 s during the second injection. In addition, the second MAB was injected alone in a separate cycle.

The trimer immobilization levels and MAB concentrations were optimized previously to yield maximum self-competition. Rabbit MABs (05A1, 05A2, and 05A3), PGT121, PGT151, and ACS202 showed 5 to 15% residual binding at a concentration of 1 μM and a trimer density of 500 RU, whereas VRC01 and 35O22 self-competed (15 to 20% residual binding) at a concentration of 1.5 μM and a density of \sim 250 RU of AMC008 SOSIP.v4.2 trimer. Those MAB concentrations were used thereafter in the cross-competitions; for rabbit MABs and VRC01 or 35O22, the trimer was captured to a level of 250 RU, whereas the other Abs (PGT121, PGT151, and ACS202) were done at a trimer capture level of 500 RU. The residual binding was calculated as follows: [(response difference at 200 s for the second Ab)/(response difference at 200 s for the same, second Ab when injected as a single Ab in a separate cycle)] \times 100 (%). Significance was determined by a one-way ANOVA multiple-comparison test (Prism) comparing the sample without competitor to the corresponding sample with competitor present.

Full-length SOSIP binding experiment. Surface-expressed full-length AMC008.v4.2 SOSIP Env trimers were obtained by cotransfection of 10 μg gp160 SOSIP expression plasmid (39) and 2.5 μg furin expression plasmid into 1.75×10^6 cells/ml HEK293F cells, as described above. At 60 to 65 h posttransfection, cells were spun down at $4,000 \times g$. 293F cells (1×10^5) were added to each well of serially diluted MABs and incubated for 2 h on ice. Cells were washed twice with PBS and subsequently stained in a volume of 20 μl containing 1:70 Alexa 647 (2 mg/ml)-conjugated mouse anti-human IgG (for 2G12 and PGT145 controls) (Invitrogen) or 1:70 PE (0.1 mg/ml)-conjugated mouse anti-rabbit IgG (Southern Biotech). Cells were stained for 45 min on ice, covered in foil, and subsequently washed with PBS and resuspended in 100 μl PBS and analyzed using a FACSCanto II analyzer (BD). Maximum mean fluorescent intensity (MFI) was calculated and plotted for each of the samples.

Data availability. Antibody sequences are available on request to the corresponding author. Variable domain sequences of heavy and light chains were uploaded in GenBank under accession numbers [MZ170096](#), [MZ170095](#), [MZ170094](#), and [MZ170097](#) for NABs 05A1, 05A2, 05A3, and 07A1, respectively.

ACKNOWLEDGMENTS

This work was supported by the HIV Vaccine Research and Design (HIVRAD) program (P01 AI110657 to A.B.W., J.P.M., P.J.K., and R.W.S.), by the Bill and Melinda Gates Foundation through the Collaboration for AIDS Vaccine Discovery (CAVD) (grants OPP1111923, OPP1132237, and INV-002022 to R.W.S. and grant OPP1170236 to A.B.W.), by the European Union's Horizon 2020 research and innovation program (grant agreement 681137 to R.W.S.), and by the NIH (grant AI36082 to J.P.M. and P.J.K.). Support was also obtained from an equipment grant from the Fondation Dornier, Vaduz (to R.W.S. and M.J.G.). R.W.S. is a recipient of a Vici grant from the Netherlands Organization for Scientific Research (NWO). M. J.G. is a recipient of an AMC Fellowship and a Mathilde Krim Fellowship from the American Foundation for AIDS Research (amfAR) (109514-61-RKVA). The Amsterdam Cohort Studies (ACS) on HIV infection and AIDS, a collaboration between the Amsterdam Health Service, the Academic Medical Center of the University of Amsterdam, Sanquin Blood Supply Foundation, and the Jan van Goyen Clinic, are part of The Netherlands HIV Monitoring Foundation and are financially supported by the Center for Infectious Disease Control of the Netherlands National Institute for Public Health and the Environment.

The electron microscopy data were collected at Electron Microscopy Facility of the Scripps Research Institute. We declare no conflicts of interest.

REFERENCES

- Dubrovskaya V, Tran K, Ozorowski G, Guenaga J, Wilson R, Bale S, Cottrell CA, Turner HL, Seabright G, O'Dell S, Torres JL, Yang L, Feng Y, Leaman DP, Vázquez Bernat N, Liban T, Louder M, McKee K, Bailer RT, Movsesyan A, Doria-Rose NA, Pancera M, Karlsson Hedestam GB, Zwick MB, Crispin M, Mascola JR, Ward AB, Wyatt RT. 2019. Vaccination with glycan-modified HIV NFL envelope trimer-liposomes elicits broadly neutralizing antibodies to multiple sites of vulnerability. *Immunity* 51:915–929.e7. <https://doi.org/10.1016/j.immuni.2019.10.008>.
- Brouwer PJM, Antanasijevic A, Berndsen Z, Yasmeen A, Fiala B, Bijl TPL, Bontjer I, Bale JB, Sheffler W, Allen JD, Schorcht A, Burger JA, Camacho M, Ellis D, Cottrell CA, Behrens AJ, Catalano M, del Moral-Sánchez I, Ketas TJ, LaBranche C, van Gils MJ, Sliepen K, Stewart LJ, Crispin M, Montefiori DC, Baker D, Moore JP, Klasse PJ, Ward AB, King NP, Sanders RW. 2019. Enhancing and shaping the immunogenicity of native-like HIV-1 envelope trimers with a two-component protein nanoparticle. *Nat Commun* 10:4272. <https://doi.org/10.1038/s41467-019-12080-1>.
- Rutten L, Lai YT, Blokland S, Truan D, Bisschop IJM, Strokappe NM, Koornneef A, van Manen D, Chuang GY, Farney SK, Schuitemaker H, Kwong PD, Langedijk JPM. 2018. A Universal approach to optimize the folding and stability of prefusion-closed HIV-1 envelope trimers. *Cell Rep* 23:584–595. <https://doi.org/10.1016/j.celrep.2018.03.061>.
- Derking R, Ozorowski G, Sliepen K, Yasmeen A, Cupo A, Torres JL, Julien JP, Lee JH, van Montfort T, de Taeye SW, Connors M, Burton DR, Wilson IA, Klasse PJ, Ward AB, Moore JP, Sanders RW. 2015. Comprehensive antigenic map of a cleaved soluble HIV-1 envelope trimer. *PLoS Pathog* 11:e1004767-22. <https://doi.org/10.1371/journal.ppat.1004767>.
- Sanders RW, Vesanan M, Schuelke N, Master A, Schiffner L, Kalyanaraman R, Paluch M, Berkhout B, Maddon PJ, Olson WC, Lu M, Moore JP. 2002. Stabilization of the soluble, cleaved, trimeric form of the envelope glycoprotein complex of human immunodeficiency virus type 1. *J Virol* 76:8875–8889. <https://doi.org/10.1128/jvi.76.17.8875-8889.2002>.
- Sanders RW, Van Gils MJ, Derking R, Sok D, Ketas TJ, Burger JA, Ozorowski G, Cupo A, Simonich C, Goo L, Arendt H, Kim HJ, Lee JH, Pugach P, Williams M, Debnath G, Moldt B, Van Breemen MJ, Isik G, Medina-Ramírez M, Back JW, Koff WC, Julien JP, Rakasz EG, Seaman MS, Guttman M, Lee KK, Klasse PJ, LaBranche C, Schief WR, Wilson IA, Overbaugh J, Burton DR, Ward AB, Montefiori DC, Dean H, Moore JP. 2015. HIV-1 neutralizing antibodies induced by native-like envelope trimers. *Science* (80-) 349: aac4223–349. <https://doi.org/10.1126/science.aac4223>.
- Hladik F, McElrath MJ. 2008. Setting the stage: host invasion by HIV. *Nat Rev Immunol* 8:447–457. <https://doi.org/10.1038/nri2302>.
- Sanders RW, Derking R, Cupo A, Julien JP, Yasmeen A, de Val N, Kim HJ, Blattner C, de la Peña AT, Korzun J, Golabek M, de los Reyes K, Ketas TJ, van Gils MJ, King CR, Wilson IA, Ward AB, Klasse PJ, Moore JP. 2013. A next-generation cleaved, soluble HIV-1 Env trimer, BG505 SOSIP.664 gp140, expresses multiple epitopes for broadly neutralizing but not non-neutralizing antibodies. *PLoS Pathog* 9:e1003618. <https://doi.org/10.1371/journal.ppat.1003618>.
- Torrents de la Peña A, de Taeye SW, Sliepen K, LaBranche CC, Burger JA, Schermer EE, Montefiori DC, Moore JP, Klasse PJ, Sanders RW. 2018. Immunogenicity in rabbits of HIV-1 SOSIP trimers from clades A, B, and C, given individually, sequentially, or in combination. *J Virol* 92:e01957-17. <https://doi.org/10.1128/JVI.01957-17>.
- de Taeye SW, Ozorowski G, Torrents de la Peña A, Guttman M, Julien J-P, van den Kerkhof TLGM, Burger JA, Pritchard LK, Pugach P, Yasmeen A, Crampton J, Hu J, Bontjer I, Torres JL, Arendt H, DeStefano J, Koff WC, Schuitemaker H, Eggink D, Berkhout B, Dean H, LaBranche C, Crotty S, Crispin M, Montefiori DC, Klasse PJ, Lee KK, Moore JP, Wilson IA, Ward AB, Sanders RW. 2015. Immunogenicity of stabilized HIV-1 envelope trimers with reduced exposure of non-neutralizing epitopes. *Cell* 163:1702–1715. <https://doi.org/10.1016/j.cell.2015.11.056>.
- Pauthner M, Havenar-Daughton C, Sok D, Nkolola JP, Bastidas R, Boopathy AV, Carnathan DG, Chandrashekar A, Cirelli KM, Cottrell CA, Eroshkin AM, Guenaga J, Kaushik K, Kulp DW, Liu J, McCoy LE, Oom AL, Ozorowski G, Post KW, Sharma SK, Steichen JM, de Taeye SW, Tokatlian T, Torrents de la Peña A, Butera ST, LaBranche CC, Montefiori DC, Silvestri G, Wilson IA, Irvine DJ, Sanders RW, Schief WR, Ward AB, Wyatt RT, Barouch DH, Crotty S, Burton DR. 2017. Elicitation of robust tier 2 neutralizing antibody responses in nonhuman primates by HIV envelope trimer immunization using optimized approaches. *Immunity* 46:1073–1088.e6. <https://doi.org/10.1016/j.immuni.2017.05.007>.
- Bale S, Martiné A, Wilson R, Behrens AJ, Le Fourn V, de Val N, Sharma SK, Tran K, Torres JL, Girod PA, Ward AB, Crispin M, Wyatt RT. 2018. Cleavage-independent HIV-1 trimers from CHO cell lines elicit robust autologous tier 2 neutralizing antibodies. *Front Immunol* 9:1116. <https://doi.org/10.3389/fimmu.2018.01116>.
- Burton DR. 2017. What are the most powerful immunogen design vaccine strategies? Reverse vaccinology 2.0 shows great promise. *Cold Spring Harb Perspect Biol* 9:a030262. <https://doi.org/10.1101/cshperspect.a030262>.
- van Haaren MM, van den Kerkhof TLGM, van Gils MJ. 2017. Natural infection as a blueprint for rational HIV vaccine design. *Hum Vaccin Immunother* 13:229–236. <https://doi.org/10.1080/21645515.2016.1232785>.
- Klasse PJ, Ketas TJ, Cottrell CA, Ozorowski G, Debnath G, Camara D, Francomano E, Pugach P, Ringe RP, LaBranche CC, van Gils MJ, Bricault CA, Barouch DH, Crotty S, Silvestri G, Kasturi S, Pulendran B, Wilson IA, Montefiori DC, Sanders RW, Ward AB, Moore JP. 2018. Epitopes for neutralizing antibodies induced by HIV-1 envelope glycoprotein BG505 SOSIP trimers in rabbits and macaques. *PLoS Pathog* 14:e1006913. <https://doi.org/10.1371/journal.ppat.1006913>.
- McCoy LE, van Gils MJ, Ozorowski G, Messmer T, Briney B, Voss JE, Kulp DW, Macauley MS, Sok D, Pauthner M, Menis S, Cottrell CA, Torres JL, Hsueh J, Schief WR, Wilson IA, Ward AB, Sanders RW, Burton DR. 2016. Holes in the glycan shield of the native HIV envelope are a target of trimer-elicited neutralizing antibodies. *Cell Rep* 16:2327–2338. <https://doi.org/10.1016/j.celrep.2016.07.074>.
- Cottrell CA, van Schooten J, Bowman CA, Yuan M, Oyen D, Shin M, Morpurgo R, van der Woude P, van Breemen M, Torres JL, Patel R, Gross J, Sewall LM, Coppes J, Ozorowski G, Nogal B, Sok D, Rakasz EG, Labranche C, Vigdorovich V, Christley S, Carnathan DG, Sather DN, Montefiori D, Silvestri G, Burton DR, Moore JP, Wilson IA, Sanders RW, Ward AB, van Gils MJ. 2020. Mapping the immunogenic landscape of near-native HIV-1 envelope trimers in non-human primates. *PLoS Pathog* 16:e1008753. <https://doi.org/10.1371/journal.ppat.1008753>.
- Ringe RP, Pugach P, Cottrell CA, LaBranche CC, Seabright GE, Ketas TJ, Ozorowski G, Kumar S, Schorcht A, van Gils MJ, Crispin M, Montefiori DC, Wilson IA, Ward AB, Sanders RW, Klasse PJ, Moore JP. 2018. Closing and opening holes in the glycan shield of HIV-1 envelope glycoprotein SOSIP trimers can redirect the neutralizing antibody response to the newly unmasked epitopes. *J Virol* 93:e01656-18. <https://doi.org/10.1128/JVI.01656-18>.
- Nogal B, Bianchi M, Cottrell CA, Kirchdoerfer RN, Sewall LM, Turner HL, Zhao F, Sok D, Burton DR, Hangartner L, Ward AB. 2019. Mapping polyclonal antibody responses in non-human primates vaccinated with HIV Env trimer subunit vaccines. *bioRxiv* 833715. <https://doi.org/10.1101/833715>.
- Bianchi M, Turner HL, Nogal B, Cottrell CA, Oyen D, Pauthner M, Bastidas R, Nedellec R, McCoy LE, Wilson IA, Burton DR, Ward AB, Hangartner L. 2018. Electron-microscopy-based epitope mapping defines specificities of polyclonal antibodies elicited during HIV-1 BG505 envelope trimer immunization. *Immunity* 49:288–300.e8. <https://doi.org/10.1016/j.immuni.2018.07.009>.
- Yasmeen A, Ringe R, Derking R, Cupo A, Julien JP, Burton DR, Ward AB, Wilson IA, Sanders RW, Moore JP, Klasse PJ. 2014. Differential binding of neutralizing and non-neutralizing antibodies to native-like soluble HIV-1 Env trimers, uncleaved Env proteins, and monomeric subunits. *Retrovirology* 11:41. <https://doi.org/10.1186/1742-4690-11-41>.
- Steckbeck JD, Orlov I, Chow A, Grieser H, Miller K, Bruno J, Robinson JE, Montelaro RC, Cole KS. 2005. Kinetic rates of antibody binding correlate with neutralization sensitivity of variant simian immunodeficiency virus strains. *J Virol* 79:12311–12320. <https://doi.org/10.1128/JVI.79.19.12311-12320.2005>.
- Wibmer CK, Gorman J, Anthony CS, Mkhize NN, Druz A, York T, Schmidt SD, Labuschagne P, Louder MK, Bailer RT, Abdoal Karim SS, Mascola JR, Williamson C, Moore PL, Kwong PD, Morris L. 2016. Structure of an N276-dependent HIV-1 neutralizing antibody targeting a rare V5 glycan hole adjacent to the CD4 binding site. *J Virol* 90:10220–10235. <https://doi.org/10.1128/JVI.01357-16>.
- Pan R, Sampson JM, Chen Y, Vaine M, Wang S, Lu S, Kong X-P. 2013. Rabbit Anti-HIV-1 monoclonal antibodies raised by immunization can mimic the antigen-binding modes of antibodies derived from HIV-1-infected humans. *J Virol* 87:10221–10231. <https://doi.org/10.1128/JVI.00843-13>.
- Voss JE, Andrabi R, McCoy LE, de Val N, Fuller RP, Messmer T, Su CY, Sok D, Khan SN, Garces F, Pritchard LK, Wyatt RT, Ward AB, Crispin M, Wilson IA, Burton DR. 2017. Elicitation of neutralizing antibodies targeting the V2 apex of the HIV envelope trimer in a wild-type animal model. *Cell Rep* 21:222–235. <https://doi.org/10.1016/j.celrep.2017.09.024>.

26. Duan H, Chen X, Boyington JC, Cheng C, Zhang Y, Jafari AJ, Stephens T, Tsybovsky Y, Kalyuzhnyi O, Zhao P, Menis S, Nason MC, Normandin E, Mukhamedova M, DeKosky BJ, Wells L, Schief WR, Tian M, Alt FW, Kwong PD, Mascola JR. 2018. Glycan masking focuses immune responses to the HIV-1 CD4-binding site and enhances elicitation of VRC01-class precursor antibodies. *Immunity* 49:301–311.e5. <https://doi.org/10.1016/j.immuni.2018.07.005>.
27. Hessel AJ, Powell R, Jiang X, Luo C, Weiss S, Dussupt V, Itri V, Fox A, Shapiro MB, Pandey S, Cheever T, Fuller DH, Park B, Krebs SJ, Totrov M, Haigwood NL, Kong XP, Zolla-Pazner S. 2019. Multimeric epitope-scaffold HIV vaccines target V1V2 and differentially tune polyfunctional antibody responses. *Cell Rep* 28:877–895.e6. <https://doi.org/10.1016/j.celrep.2019.06.074>.
28. Rantalainen K, Berndsen ZT, Antanasijevic A, Schiffner T, Zhang X, Lee WH, Torres JL, Zhang L, Irimia A, Copps J, Zhou KH, Kwon YD, Law WH, Schramm CA, Verardi R, Krebs SJ, Kwong PD, Doria-Rose NA, Wilson IA, Zwick MB, Yates JR, Schief WR, Ward AB. 2020. HIV-1 envelope and MPER antibody structures in lipid assemblies. *Cell Rep* 31:107583. <https://doi.org/10.1016/j.celrep.2020.107583>.
29. Lee JH, Leaman DP, Kim AS, Torrents De La Penã A, Slieden K, Yasmeen A, Derking R, Ramos A, De Taeye SW, Ozorowski G, Klein F, Burton DR, Nussenzweig MC, Poignard P, Moore JP, Klasse PJ, Sanders RW, Zwick MB, Wilson IA, Ward AB. 2015. Antibodies to a conformational epitope on gp41 neutralize HIV-1 by destabilizing the Env spike. *Nat Commun* 6:8167. <https://doi.org/10.1038/ncomms9167>.
30. Kong L, Lee JH, Doores KJ, Murin CD, Julien JP, McBride R, Liu Y, Marozsan A, Cupo A, Klasse PJ, Hoffenberg S, Caulfield M, King CR, Hua Y, Le KM, Khayat R, Deller MC, Clayton T, Tien H, Feizi T, Sanders RW, Paulson JC, Moore JP, Stanfield RL, Burton DR, Ward AB, Wilson IA. 2013. Supersite of immune vulnerability on the glycosylated face of HIV-1 envelope glycoprotein gp120. *Nat Struct Mol Biol* 20:796–803. <https://doi.org/10.1038/nsmb.2594>.
31. Pejchal R, Doores KJ, Walker LM, Khayat R, Huang PS, Wang SK, Stanfield RL, Julien JP, Ramos A, Crispin M, Depetris R, Katpally U, Marozsan A, Cupo A, Malveste S, Liu Y, McBride R, Ito Y, Sanders RW, Ogohara C, Paulson JC, Feizi T, Scanlan CN, Wong CH, Moore JP, Olson WC, Ward AB, Poignard P, Schief WR, Burton DR, Wilson IA. 2011. A potent and broad neutralizing antibody recognizes and penetrates the HIV glycan shield. *Science* 334:1097–1103. <https://doi.org/10.1126/science.1213256>.
32. Lavinder JJ, Hoi KH, Reddy ST, Wine Y, Georgiou G. 2014. Systematic characterization and comparative analysis of the rabbit immunoglobulin repertoire. *PLoS One* 9:e101322-11. <https://doi.org/10.1371/journal.pone.0101322>.
33. Kodangattil S, Huard C, Ross C, Li J, Gao H, Mascioni A, Hodawadekar S, Naik S, Min-Debartolo J, Visintin A, Almagro JC. 2014. The functional repertoire of rabbit antibodies and antibody discovery via next-generation sequencing. *MAbs* 6:628–636. <https://doi.org/10.4161/mabs.28059>.
34. Van Gils MJ, Van Den Kerkhof TLGM, Ozorowski G, Cottrell CA, Sok D, Pauthner M, Pallesen J, De Val N, Yasmeen A, De Taeye SW, Schorch A, Gumbs S, Johanna I, Saye-Francisco K, Liang CH, Landais E, Nie X, Pritchard LK, Crispin M, Kelsoe G, Wilson IA, Schuitemaker H, Klasse PJ, Moore JP, Burton DR, Ward AB, Sanders RW. 2017. An HIV-1 antibody from an elite neutralizer implicates the fusion peptide as a site of vulnerability. *Nat Microbiol* 2:423–426. <https://doi.org/10.1038/nmicrobiol.2016.199>.
35. deCamp A, Hraber P, Bailer RT, Seaman MS, Ochsenaubauer C, Kappes J, Gottardo R, Edlefsen P, Self S, Tang H, Greene K, Gao H, Daniell X, Sartzotti-Kelsoe M, Gorny MK, Zolla-Pazner S, LaBranche CC, Mascola JR, Korber BT, Montefiori DC. 2014. Global panel of HIV-1 Env reference strains for standardized assessments of vaccine-elicited neutralizing antibodies. *J Virol* 88:2489–2507. <https://doi.org/10.1128/JVI.02853-13>.
36. Slieden K, Han BW, Bontjer I, Mooij P, Garcés F, Behrens AJ, Rantalainen K, Kumar S, Sarkar A, Brouwer PJM, Hua Y, Tolazzi M, Schermer E, Torres JL, Ozorowski G, van der Woude P, de la Peña AT, van Breemen MJ, Camacho-Sánchez JM, Burger JA, Medina-Ramírez M, González N, Alcami J, LaBranche C, Scarlatti G, van Gils MJ, Crispin M, Montefiori DC, Ward AB, Koopman G, Moore JP, Shattock RJ, Bogers WM, Wilson IA, Sanders RW. 2019. Structure and immunogenicity of a stabilized HIV-1 envelope trimer based on a group-M consensus sequence. *Nat Commun* 10:2355. <https://doi.org/10.1038/s41467-019-10262-5>.
37. Falkowska E, Le KM, Ramos A, Doores KJ, Lee JH, Blattner C, Ramirez A, Derking R, van Gils MJ, Liang C-H, McBride R, von Bredow B, Shivatare SS, Wu C-Y, Chan-Hui P-Y, Liu Y, Feizi T, Zwick MB, Koff WC, Seaman MS, Swiderek K, Moore JP, Evans D, Paulson JC, Wong C-H, Ward AB, Wilson IA, Sanders RW, Poignard P, Burton DR. 2014. Broadly neutralizing HIV antibodies define a glycan-dependent epitope on the prefusion conformation of gp41 on cleaved envelope trimers. *Immunity* 40:657–668. <https://doi.org/10.1016/j.immuni.2014.04.009>.
38. Blattner C, Lee JH, Slieden K, Derking R, Falkowska E, de la Peña AT, Cupo A, Julien J-P, van Gils M, Lee PS, Peng W, Paulson JC, Poignard P, Burton DR, Moore JP, Sanders RW, Wilson IA, Ward AB. 2014. Structural delineation of a quaternary, cleavage-dependent epitope at the gp41-gp120 interface on intact HIV-1 env trimers. *Immunity* 40:669–680. <https://doi.org/10.1016/j.immuni.2014.04.008>.
39. Torrents de la Peña A, Rantalainen K, Cottrell CA, Allen JD, van Gils MJ, Torres JL, Crispin M, Sanders RW, Ward AB. 2019. Similarities and differences between native HIV-1 envelope glycoprotein trimers and stabilized soluble trimer mimetics. *PLoS Pathog* 15:e1007920. <https://doi.org/10.1371/journal.ppat.1007920>.
40. Mage RG, Lanning D, Knight KL. 2006. B cell and antibody repertoire development in rabbits: the requirement of gut-associated lymphoid tissues. *Dev Comp Immunol* 30:137–153. <https://doi.org/10.1016/j.dci.2005.06.017>.
41. Medina-Ramírez M, Garcés F, Escolano A, Skog P, de Taeye SW, Del Moral-Sanchez I, McGuire AT, Yasmeen A, Behrens AJ, Ozorowski G, van den Kerkhof TLGM, Freund NT, Dosenovic P, Hua Y, Gitlin AD, Cupo A, van der Woude P, Golabek M, Slieden K, Blane T, Kootstra N, van Breemen MJ, Pritchard LK, Stanfield RL, Crispin M, Ward AB, Stamatatos L, Klasse PJ, Moore JP, Nemazee D, Nussenzweig MC, Wilson IA, Sanders RW. 2017. Design and crystal structure of a native-like HIV-1 envelope trimer that engages multiple broadly neutralizing antibody precursors *in vivo*. *J Exp Med* 214:2573–2590. <https://doi.org/10.1084/jem.20161160>.
42. Hessel AJ, Malherbe DC, Pissani F, McBurney S, Krebs SJ, Gomes M, Pandey S, Sutton WF, Burwitz BJ, Gray M, Robins H, Park BS, Sacha JB, LaBranche CC, Fuller DH, Montefiori DC, Stamatatos L, Sather DN, Haigwood NL. 2016. Achieving potent autologous neutralizing antibody responses against tier 2 HIV-1 viruses by strategic selection of envelope immunogens. *J Immunol* 196:3064–3078. <https://doi.org/10.4049/jimmunol.1500527>.
43. Ozorowski G, Pallesen J, De Val N, Lyumkis D, Cottrell CA, Torres JL, Copps J, Stanfield RL, Cupo A, Pugach P, Moore JP, Wilson IA, Ward AB. 2017. Open and closed structures reveal allostery and pliability in the HIV-1 envelope spike. *Nature* 547:360–361. <https://doi.org/10.1038/nature23010>.
44. Lee JH, Ozorowski G, Ward AB. 2016. Cryo-EM structure of a native, fully glycosylated, cleaved HIV-1 envelope trimer. *Science* 351:1043–1048. <https://doi.org/10.1126/science.aad2450>.
45. Ke Z, Oton J, Qu K, Cortese M, Zila V, McKeane L, Nakane T, Zivanov J, Neufeldt CJ, Cerikan B, Lu JM, Peukes J, Xiong X, Kräusslich HG, Scheres SHW, Bartenschlager R, Briggs JAG. 2020. Structures and distributions of SARS-CoV-2 spike proteins on intact virions. *Nature* 588:498–502. <https://doi.org/10.1038/s41586-020-2665-2>.
46. Klasse PJ. 2014. Neutralization of virus infectivity by antibodies: old problems in new perspectives. *Adv Biol* 2014:157895. <https://doi.org/10.1155/2014/157895>.
47. Torrents de la Peña A, Julien JP, de Taeye SW, Garcés F, Guttman M, Ozorowski G, Pritchard LK, Behrens AJ, Go EP, Burger JA, Schermer EE, Slieden K, Ketas TJ, Pugach P, Yasmeen A, Cottrell CA, Torres JL, Vavourakis CD, van Gils MJ, LaBranche C, Montefiori DC, Desaire H, Crispin M, Klasse PJ, Lee KK, Moore JP, Ward AB, Wilson IA, Sanders RW. 2017. Improving the immunogenicity of native-like HIV-1 envelope trimers by hyperstabilization. *Cell Rep* 20:1805–1817. <https://doi.org/10.1016/j.celrep.2017.07.077>.
48. Guenaga J, Dubrovskaya V, de Val N, Sharma SK, Carrette B, Ward AB, Wyatt RT. 2016. Structure-guided redesign increases the propensity of HIV Env to generate highly stable soluble trimers. *J Virol* 90:2806–2817. <https://doi.org/10.1128/JVI.02652-15>.
49. Kulp DW, Steichen JM, Pauthner M, Hu X, Schiffner T, Liguori A, Cottrell CA, Havenar-Daughton C, Ozorowski G, Georgeson E, Kalyuzhnyi O, Willis JR, Kubitz M, Adachi Y, Reiss SM, Shin M, De Val N, Ward AB, Crotty S, Burton DR, Schief WR. 2017. Structure-based design of native-like HIV-1 envelope trimers to silence non-neutralizing epitopes and eliminate CD4 binding. *Nat Commun* 8:1655. <https://doi.org/10.1038/s41467-017-01549-6>.
50. Binley JM, Sanders RW, Clas B, Schuelke N, Master A, Guo Y, Kajumo F, Anselma DJ, Maddon PJ, Olson WC, Moore JP. 2000. A recombinant human immunodeficiency virus type 1 envelope glycoprotein complex stabilized by an intermolecular disulfide bond between the gp120 and gp41 subunits is an antigenic mimic of the trimeric virion-associated structure. *J Virol* 74:627–643. <https://doi.org/10.1128/jvi.74.2.627-643.2000>.
51. Julien JP, Lee JH, Ozorowski G, Hua Y, De La Peña AT, De Taeye SW, Nieuwsma T, Cupo A, Yasmeen A, Golabek M, Pugach P, Klasse PJ, Moore

- JP, Sanders RW, Ward AB, Wilson IA. 2015. Design and structure of two HIV-1 clade C SOSIP.664 trimers that increase the arsenal of native-like Env immunogens. *Proc Natl Acad Sci U S A* 112:11947–11952. <https://doi.org/10.1073/pnas.1507793112>.
52. Pugach P, Ozorowski G, Cupo A, Ringe R, Yasmeen A, de Val N, Derking R, Kim HJ, Korzun J, Golabek M, de los Reyes K, Ketas TJ, Julien J-P, Burton DR, Wilson IA, Sanders RW, Klasse PJ, Ward AB, Moore JP. 2015. A native-like SOSIP.664 trimer based on an HIV-1 subtype B *env* gene. *J Virol* 89:3380–3395. <https://doi.org/10.1128/JVI.03473-14>.
53. Suloway C, Pulokas J, Fellmann D, Cheng A, Guerra F, Quispe J, Stagg S, Potter CS, Carragher B. 2005. Automated molecular microscopy: the new Legimon system. *J Struct Biol* 151:41–60. <https://doi.org/10.1016/j.jsb.2005.03.010>.
54. Lander GC, Stagg SM, Voss NR, Cheng A, Fellmann D, Pulokas J, Yoshioka C, Irving C, Mulder A, Lau PW, Lyumkis D, Potter CS, Carragher B. 2009. Appion: an integrated, database-driven pipeline to facilitate EM image processing. *J Struct Biol* 166:95–102. <https://doi.org/10.1016/j.jsb.2009.01.002>.
55. Voss NR, Yoshioka CK, Radermacher M, Potter CS, Carragher B. 2009. DoG Picker and TiltPicker: software tools to facilitate particle selection in single particle electron microscopy. *J Struct Biol* 166:205–213. <https://doi.org/10.1016/j.jsb.2009.01.004>.
56. Scheres SHW. 2012. RELION: implementation of a Bayesian approach to cryo-EM structure determination. *J Struct Biol* 180:519–530. <https://doi.org/10.1016/j.jsb.2012.09.006>.
57. Pettersen EF, Goddard TD, Huang CC, Couch GS, Greenblatt DM, Meng EC, Ferrin TE. 2004. UCSF Chimera—a visualization system for exploratory research and analysis. *J Comput Chem* 25:1605–1612. <https://doi.org/10.1002/jcc.20084>.
58. Wagh K, Kreider EF, Li Y, Barbian HJ, Learn GH, Giorgi E, Hraber PT, Decker TG, Smith AG, Gondim MV, Gillis L, Wandzilak J, Chuang GY, Rawi R, Cai F, Pellegrino P, Williams I, Overbaugh J, Gao F, Kwong PD, Haynes BF, Shaw GM, Borrow P, Seaman MS, Hahn BH, Korber B. 2018. Completeness of HIV-1 envelope glycan shield at transmission determines neutralization breadth. *Cell Rep* 25:893–908.e7. <https://doi.org/10.1016/j.celrep.2018.09.087>.